TÉCNICO LISBOA

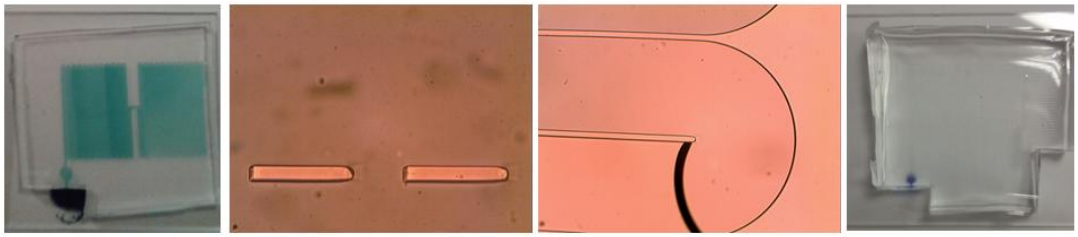

Capillary Biochip for point of use biomedical application

Joana de Carvalho Rodrigues Mesquita Chim

Thesis to obtain the Master of Science Degree in

Biomedical Engineering

Supervisors: Prof. João Pedro Estrela Rodrigues Conde
Dr. João Garcia da Fonseca

Examination Committee

Chairperson: Prof. Raúl Daniel Lavado Carneiro Martins
Supervisors: Prof. João Pedro Estrela Rodrigues Conde
Members of the Committee: Dr. Nuno Alexandre Esteves Reis
Prof. Frederico Castelo Alves Ferreira

November 2015

Não tenhamos pressa, mas não percamos tempo.

José Saramago

Acknowledgments

Terminada esta etapa do meu percurso académico, gostaria de agradecer a todas as pessoas que me acompanharam e apoiaram no decorrer deste projecto.

Um primeiro agradecimento é dirigido ao Prof. João Pedro Conde por me ter aceite para este desafio e por toda a orientação que me deu nestes meses de trabalho. Ao co-orientador Dr. João Garcia da Fonseca segue também um agradecimento pela disponibilidade que demonstrou em mostrar o seu trabalho e pelas trocas de ideias que enriqueceram este projecto.

Gostaria também de expressar um obrigado aos meus colegas do INESC-MN, por toda a motivação, ajuda e partilha de opiniões e sugestões. Em especial, ao Rúben Soares, por ter sempre estado disponível para me ajudar, esclarecer dúvidas e ensinar novas abordagens de trabalho. Para a Virgínia Soares segue também um obrigado, por me ter ajudado sempre que foi preciso. Gostaria ainda de mencionar a Dra. Virgínia Chu por todas as sugestões dadas, que me fizeram pensar de forma mais crítica. Por fim, à Catarina, à Rita e ao Eduardo pelos cafés e pelas gargalhadas que acompanharam os momentos de laboratório.

Como não poderia deixar de ser, um grande obrigado a todos os meus amigos, pelos almoços, partilha de experiências, de conselhos e especialmente pela sua amizade. Foi uma alegria partilhar convosco este percurso de 5anos.

Por fim, mas em primeiro lugar, à minha família, aos meus pais e à minha irmã. Obrigado por toda a motivação, palavras de ânimo e por todo o carinho, que me trouxeram a este momento tão especial.

Abstract

Microfluidic devices have become an attractive technology in terms of point of care use, due to reduction of sample and reagents consumption, time and also costs of analysis. These devices allow to simplify laboratory protocols and perform them in a single chip of small dimensions. However, some of the devices developed require combining the chip with external equipment that can be complex for handling and difficult the PoC application.

In order to solve these issues, capillary chips come into play. Capillary-driven microfluidics introduce a wide range of benefits, including being user friendly and portability, owed to the fact that fluid flow is only controlled by the surface wetting properties of the device. Taking advantage of these benefits this work proposes a capillary chip for a specific biomedical application, namely an immunoassay or the detection of the mycotoxin OTA.

PDMS and glass were the materials chosen for the fabrication of the capillary chips. In addition an intensive study of the work conditions is presented. Namely the effect that different capillary pumps can have in fluid motion. Since surface properties are determinant in capillarity, the influence of the UV/Ozone treatment was also tested. In terms of application, the chip was shown to be capable of providing the required conditions for performing the OTA immunoassay. Demonstrating to be sensitive enough to allow the detection of OTA concentrations within the regulatory limits.

The capillary chip proposed in this project combines the requirements for a PoC device, easy to use and portable.

Key words: capillarity; microfluidic devices; capillary pumps; surface treatment; OTA immunoassay

Resumo

Dispositivos microfluídicos têm a vindo a tornar-se uma tecnologia atractiva para sistemas de diagnóstico, devido a uma redução do consumo de amostras e reagentes, tempo e custo de análises. Estes dispositivos permitem então simplificar protocolos laboratoriais e realizá-los num único chip de dimensões reduzidas. No entanto, alguns destes dispositivos requerem a combinação destes dispositivos com equipamento externo. Assim, podem tornar-se complexo manuseá-los, dificultando a análise.

De modo a resolver estes problemas, surgem os chips capilares. Dispositivos microfluídicos baseados em capilaridade introduzem uma variedade de benefícios, incluindo serem fáceis de manusear e portáteis. Estas devem-se ao facto de que o movimento dos fluídos é apenas controlado pelas características das superfícies que compõem o dispositivo. Tomando partido destas vantagens este trabalho propõem um chip capilar para uma aplicação biomédica específica. Nomeadamente, a detecção da toxina OTA.

Os materiais escolhidos para a fabricação do chip foram PDMS e vidro. Este trabalho inclui um estudo intensivo sobre o princípio de funcionamento do dispositivo, designadamente o efeito que várias bombas capilares podem ter no movimento do fluído. Sendo as propriedades das superfícies determinantes em capilaridade a influência de um tratamento com UV/Ozono foi estudado. Em relação à aplicação, o chip demonstrou ser capaz de fornecer as condições necessárias para desenvolver um imunoensaio. Demonstrando ser sensível o suficiente para permitir a detecção das concentrações de OTA de interesse, dentro dos limites legais.

O chip capilar proposto neste trabalho combina os requisitos de acessibilidade e portabilidade importantes para dispositivos de diagnóstico.

Palavras-chave: capilaridade; dispositivos microfluídicos; bombas capilares; tratamento das superfícies; imunoensaio OTA

Contents

List of Abbreviations

BSA	Bovine serum albumin
ELISA	Enzyme-linked immunosorbent assay
icELISA	Indirect competitive enzyme-linked immunosorbent assay
HRP	Horseradish peroxidase
IPA	Isopropyl alcohol
LoC	Lab-on chip
PBS	Phosphate buffered saline
PDMS	Poly(DiMethylSiloxane)
PGMEA	Propylene glycol monomethyl ether acetate
PoC	Point-of care
OTA	Ochratoxin A
TMB	3,3',5,5'-tetramethylbenzidine
UV	Ultraviolet light

List of Figures

List of Tables

THESIS OUTLINE

This thesis is divided in four main chapters: Introduction, Methods, Results and Conclusion.

The Introduction chapter includes a brief context of the state-of-the art of microfluidic devices, and the motivation that led to the development of the capillary chip. In order to give some perspective on capillary microfluidics important concepts are described. Namely surface tension, contact angles and capillary pressure. In terms of the device, the rationale behind the choice of materials and consequent treatments of the surfaces is explained. Since the device is oriented for a specific immunodiagnostic, some fundamental notions of immunoassays and characteristics of the OTA assay are explained.

Following the trend of chapter 1, the 2nd chapter – Methods is separated in three sub-sections: Microfluidic devices fabrication, Capillary device and Biological experiments. The microfluidic chip fabrication is divided in hard mask design and fabrication, SU-8 mold and PDMS-glass microfluidic device. In order to explain how the capillary chip works, the working principle of the several components are described. To access the application of the device, the preparation of all the solutions and of the device for the immunoassay are mentioned.

Furthermore in the 3rd chapter (Results and Discussion) all the tests to which the device was subjected and the obtained results are described. The capillary chip working principle was studied in different conditions, namely behavior after treatment and flow of solutions with diverse characteristic for example viscosity. After understanding how the chip worked, the immunoassay was performed. The results for the OTA immunoassay are also explained in this chapter. In the end, and introducing a module that could facilitate handling the device, the sequential introduction of solutions is referred.

The last chapter presents the main conclusions of this thesis including future endeavors.

1 INTRODUCTION

This chapter starts with a brief context of the microfluidic research area, including the motivation that led to this thesis. Sub-section 1.3 reflects on the basic principles that rule the fluid motion within a capillary channel. Sub-section 1.4 addresses the properties of the materials that compose these devices, and surface treatments that might be necessary to perform. Since the capillary chip is designed for a specific application, basic concepts in immunoassays in microfluidic systems are assessed in sub-section 1.5.

1.1 State of the art

When ink-jet technology started to evolve, the need for handling small amounts of liquids in the nano and subnanolitre ranges forced the emergence of microfluidic study, back in the early 1950s. Later on, in 1979 a miniaturized gas chromatograph (GC) was fabricated on a silicon wafer, assuring the possibility of manipulating the propulsion of liquids within microchannels with dimensions inferior to the millimeter range. The development of microfluidic systems reached an important mark in the beginning of 1980s due to the first publications of micro valves and micropumps.[1]

These sub micrometric systems started to arouse interest, in the past two decades, due the possibility of developing new ways for fluid mixing, transport, molecular separation and concentration within miniaturized quantities of fluids.[1]

The conceptual idea behind microfluidic devices is that fluids can be manipulated in microscale devices, commonly known as miniaturized total analysis systems (μTASs). These systems introduced a wide variety of applications, from biology research to complex assay protocols and benefited from the significant reduction of sample volume, which in turn led to a decrease in cost of reagents and also provided the user with more control over the spatio-temporal dynamics of the assays conditions.[1]

In 2007, microfluidic applications were considered as a toolbox not focused for the common user and consumer, but for the academic and research community. Due to the need of *know-how* and for developing products in different fields, like biotechnology, diagnostics and pharmaceutical industries.[1] However, in fact in 2013 the microfluidic market was valued in 1.6 billion dollars. The high growth rate is due to the development of applications in gene sequencing and *in vitro* diagnostics. Several pharmaceutical companies expanded their research, in order to include devices for point-of care (PoC) diagnostics.[2]

A recent report from MarketsandMarkets refers that the evaluation of the microfluidic market for 2015 reaches the 3.1 billion dollars, and a forecast for 2020 sets a target of 7.5 billion dollars. Some of the major players include Agilent Technologies, Bio-Rad Laboratories, Abbott Laboratories and Illumina.[3],[4] Another good indicator for the appeal of this area is the increasing number of spin-off companies that emerged, trying to commercialize lab on a chip (LoC) microfluidic products.[1]

Journal articles in microfluidic devices increased significantly between 1988 and 1990 (as demonstrated in Figure 1.1). The field rapidly increased with the development of more devices, which led to a rise in patent protection. The first patent was published in 1991. The entities with a large number of patents in this area include Samsung, Philips and also the University of California. This fact shows that both industry and academia are participating in the commercialization of microfluidic devices.[4]

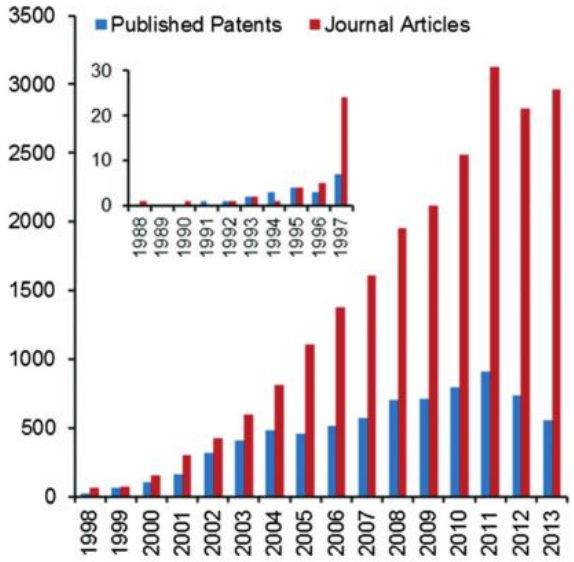

Figure 1.1 Evolution of the number of published patents and journal articles in microfluidics[4]

One successful example of a PoC device used in healthcare is the i-STAT (Abbott Laboratories). The i-STAT is a portable analyzer with disposable cartridges that detect different cardiac markers.[5] Microfluidic based systems appear when considering the need of detecting lower concentrations of a wide variety of targets.[6]

In terms of the capillary driven tests or *lateral flow assays*, the development started in the 1960s with a huge level of commercialization. Some examples of these products are the pregnancy and diabetes tests. The working principle is based in a passive liquid transport by capillary action within microchannels. These devices can be very appealing due to the possibility of performing on-site measurements in disposable and low cost devices. Therefore a significant number of assays have been developed in these platforms. However, some drawbacks arise from being too simple, for instances the fact that the assays follow a fixed process scheme, impressed in the channel design.[1]

Some of the most recent developments in capillary chips include the conception of capillary components and structures able to control fluid flow. Fluid manipulation in capillary systems has been studied by several research groups, including the microfluidics IBM group led by Delamarche.

Including the development of autonomous microfluidic capillary systems to perform immunoassays using multiple pipetting steps, back in 2002. This work introduced the concept of an autonomous capillary system, self sufficient and with a huge impact in the design of portable devices. Here it was

also established the need for valves and pumps that could distribute liquids according with their composition and application within an assay.[7,8]

The function of capillary pumps is particularly interesting for the control of accurate volumes and flow rates of the solutions. In 2007, the same group proposed a variety of designs for capillary pumps in order to encode specific flow rates, for performing immunoassays (illustrated in Figure 1.2). The geometry of these pumps was studied, in order to understand the relation with flow behavior. It was shown that their geometry has a significant impact in flow resistance and in turn in fluid flow.[9]

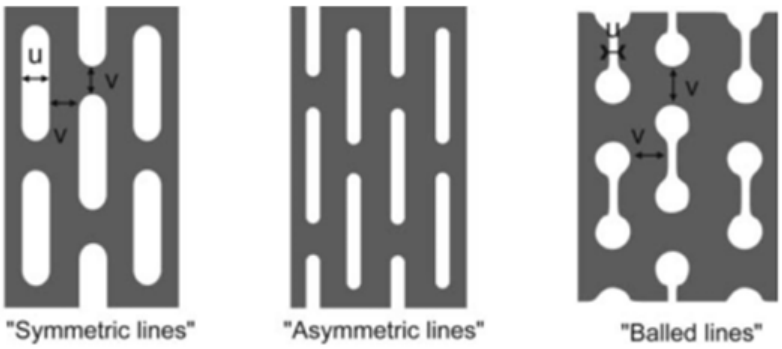

Figure 1.2 Examples of capillary pumps[9]

The creation of capillary soft valves, controlled by an abrupt expansion of the microchannels to enable stopping a fluid front, was published in 2013.[10]

Immunoassay experiments have been performed for a long time for a variety of applications, medical diagnostics, pharmaceutical, food safety and environmental analysis among others. Portable devices for immunodiagnostics are interesting for healthcare due to the possibility of decentralized and point of care testing.[11] These devices assemble a set of properties that make them attractive for diagnostic applications. The necessary sample volume is small and the devices can be portable, low cost, easy to use and require lower power consumptions. Test results can be acquired rapidly after introducing the sample. Also, since manual handling is minimal, errors and risk of contamination can be easily avoided resulting in a higher level of reproducibility.[5,12]

In 2013, Novo P. et al, proposed an autonomous capillary system, for one model of IgG-anti IgG immunoassay with fluorescence microscopy (as shown in Figure 1.3). The device only required the introduction of the solutions in the inlets. The sequential flow of solutions was assured by capillary pumps, based in previous work from Delamarche.[13,14] In the same year, the same group demonstrated an integrated analytical system that conjugated an indirect competitive ELISA in PDMS microfluidics with photodiodes for the detection of the mycotoxin OTA. The assay was performed in a non capillary straight channel.[15]

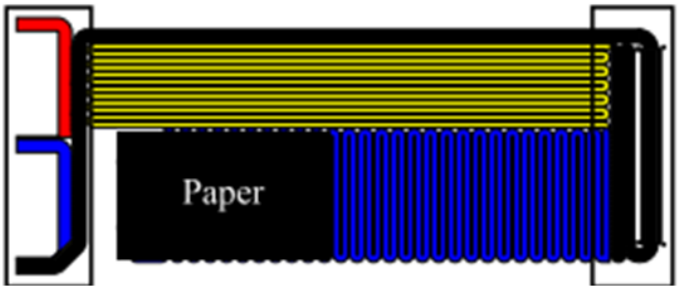

Figure 1.3 Capillary microfluidic structures[13]

In terms of the materials, the original devices were fabricated in glass and silicon. However, in 2002 Whitesides described the fabrication of microfluidics devices in PDMS. The attractiveness of this polymer is related with low cost and complexity associated with its properties. From this point on the use of this material for the production of microfluidic PoC devices increased.[16]

The main objective of this thesis is combining the development of a capillary microfluidic device in PDMS, with the detection of OTA.

1.2 Motivation

The ideal microfluidic device for PoC use should comprise several features, for instances impermeability to external liquids and not damageable when dropped in the floor from small distances. In order to allow an optical signal reading it must be composed of a transparent material. And to consider the possibility of being handled by a non-technical user the device has to be user-friendly.[17] When considering a diagnostic device, it is required to comprehend a structure that allows for the collection of the sample, analysis and calibration of the data and at last for the transmission of the result.

As the field of microfluidic PoC devices enlarges towards a more versatile technology in several fields,[18] increasing efforts have been done in order to enhance the simplicity of operation and handling of these devices. For that reason, the potential of self-filling microfluidic devices based on capillary effects emerged.[19]

Capillary chips introduce a wide range of benefits, for instances the independence of external fluidic equipment that lead to portability and produce a short time analysis. Another advantage of these devices is the small user intervention, only related with loading of solutions at the inlet of the structure. Capillary flow is controlled by surface-liquid adhesion and liquid-liquid cohesion. This way, the flow depends on surface properties and geometry.[14] Several capillary components (e.g. valves and pumps) can be incorporated into the device to manipulate the fluid flow.[5]

Regarding all the advantages that capillary devices introduce, the main motivation of this thesis was to design and fabricate a capillary chip capable of receiving several solutions, perform a specific immunoassay and transmit the result.

In the end this work proposes an autonomous capillary PDMS-glass device for general biomedical applications. In order to demonstrate its performance several tests were made, including a specific OTA immunoassay. This allows to show that by customizing the chip is possible to produce a PoC device for specific applications. The capillary chip developed only requires manipulation in the insertion of solutions and signal reading and analysis.

1.3 Fluid Dynamics

When designing and fabricating microfluidic devices is important to understand the physical phenomena that are relevant in small length scales. Since the dimension of the objects will determine the forces that dominate. In microfluidics phenomena like surface tension, contact angle and hydraulic resistance are predominant.[20]

1.3.1 Surface Tension

A molecule in the middle of a liquid is considered stable since it benefits from cohesive interactions with all its neighbors. Since each of these molecules is pulled by neighboring molecules equally in all the directions, the net force is zero. However a molecule exposed on the surface doesn't have neighboring molecules in all directions, since there are not molecules above the surface. Therefore the net force is unbalanced, and the molecules are pulled to the interior of the droplet creating an internal pressure. (As illustrated in Figure 1.4)[21]

The result of the unbalanced forces will be the contraction of the liquid in order to achieve the lowest surface free energy. The intermolecular force responsible for contracting the surface is called surface tension.[21]

Figure 1.4. Representation of unbalanced forces that create surface tension[21]

At a thermodynamic level, surface tension can be defined as the energy that needs to be supplied in order to increase by one unit the surface area. Given that interfaces between phases create added potential energy, surface tension can be considered as a force per unit length (N/m) that tends to minimize the surface area of an interface.[22] As the length scale increases its effect decreases.

1.3.2 Contact Angle

Another important concept for the understanding of capillary flows that has a close connection with surface tension is the contact angle. Contact angle can be acquired by applying a tangent line from the point where the three phases liquid/solid/gas co-exist along the liquid-gas interface

(demonstrated in Figure 1.5). The exact point where the three phases meet is called *three-phase contact line*.[21]

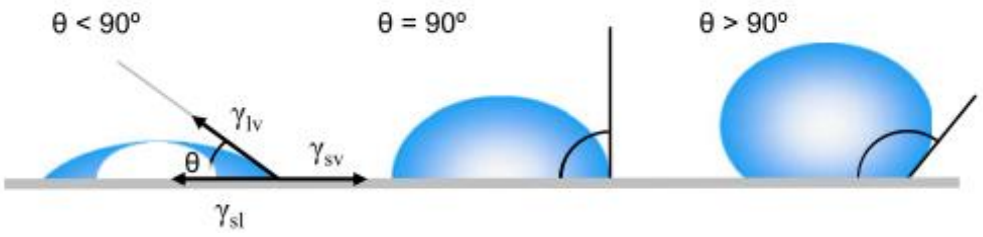

Figure 1.5. Illustration of contact angles for surfaces with different wettability properties [21]

At the equilibrium, the contact angle (θ) is determined by Young's equation that combines the surface tensions of the three interfaces involved (solid-liquid, solid-gas and liquid-gas) (Equation1). This parameter represents a relative measure of the interfacial energy of the surfaces that are in contact.[21]

$$\cos\theta = \frac{\gamma_{sg} - \gamma_{sl}}{\gamma_{lg}} \quad (1)$$

Different values of contact angles can be obtained according to the characteristics of the solid surface. This way is possible to define the wettability of a surface to a specific liquid. A certain surface can be defined as wettable if $\theta < 90°$ and non-wettable when $\theta > 90°$, where the liquid spreads or adopts a droplet form, respectively. When considering a system with a droplet of water, the solid surface can be considered hydrophilic (wettable) or hydrophobic (non-wettable) accordingly with the contact angle obtained. For a solid-liquid system the contact angle is characteristic in specific environmental conditions.[23]

1.3.3 Capillary pressure

As explained previously, a liquid in a solid surface adopts a shape with a certain curvature. This modification in conformation is associated with a pressure drop (Δp_s) at the interface. The pressure generated by a curved interface is described by the Young-Laplace equation,[24]

$$\Delta p_s = \gamma\left(\frac{1}{R_1} + \frac{1}{R_2}\right) \quad (2)$$

with R_1 and R_2 representing the radii of curvature that define the liquid's surface boundary.

Often in microchannels the liquid is constrained by two different solid surfaces instead of just one. In a microchannel with a rectangular cross section ($w \times d$), capillary forces depend on the contact angles of the liquid to each wall of the channel. Therefore, we have to consider a slight change in the Young-Laplace expression (equation2),

$$\Delta p_s = \gamma\left(\frac{cos\theta_b + cos\theta_t}{d} + \frac{cos\theta_l + cos\theta_r}{w}\right) \quad (3)$$

where θ_b, θ_t, θ_l and θ_r correspond to the contact angles of the bottom, top, left and right walls, respectively (as illustrated in Figure 1.6).[23,25]

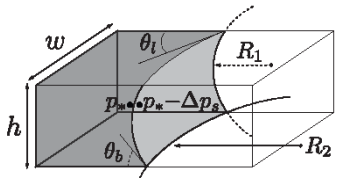

Figure 1.6 Representation of the contact angles that a fluid within a rectangular microchannel defines with the walls[26]

Capillary manipulation of microfluids can be achieved by modifying the solid-liquid interfaces or by inducing a certain gradient in the liquid-gas surface tension. The gradient in surface tensions can be of thermal, electro and chemical origin. In what respects to the modification of solid-liquid interfaces, as shown in Figure 1.7, due to the gradient in solid-liquid interfacial energy the droplet tends to move to further into the hydrophilic region.[27]

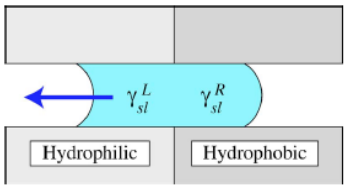

Figure 1.7. Illustration of droplet motion due to solid-liquid interfacial energy[27]

Capillary action results from the surface tension phenomenon. In this case, the liquid has the ability to flow due to the wetting properties of the surfaces that constitute the walls of the channel. Therefore capillarity allows for the fluid motion without the need of external equipment. However there is a weakness in microfluidic devices based on capillarity that has to do with the maintenance of the stability of wetting properties.[1,28] In some cases, surface tension may be the sole driving force to help the liquid flow into the chip.[29]

1.3.4 Capillary flows

There are two types of flow regimes – laminar and turbulent. A flow is considered turbulent if due its chaotic properties is not possible to predict the position of a certain particle within the stream. Whereas in a laminar regime the particles move orderly and their position can be predicted.[20] The fluid flow in a microchannel can be characterized by the Reynolds number (Re) (given in equation4),

$$Re = \frac{(inertial\ forces)}{(viscous\ forces)} = \frac{\rho v D_h}{\mu} \quad (4)$$

where ρ is the fluid density (kg/m^3), v is the fluid velocity (m/s), D_h the hydraulic diameter (m) and μ the fluid viscosity (kg/ms). This value represents the ratio between the inertial and the viscous forces, and can be considered as a measure of turbulence.[20] In microchannels due to the characteristic small dimensions the Re is very low ($Re \ll 1$) and inertial effects like gravity and turbulence can be neglected.[30]

Within microchannels the fluid flow is considered laminar, although there is another concept that can be used to define this flow. When the fluid is conducted through a long, rigid and straight channel due to a difference of pressure, the flow is defined as Poiseuille flow. In a capillary flow the fluid motion is pressure driven.[22]

In 1921, Washburn developed a correlation that entails that within a fluid channel, the fluid volumetric flow rate can be equalized to a ratio of pressure drop per resistance. This expression can be obtained from the Navier-Stokes equation by assuming a steady-state, laminar incompressible flow in a capillary system,

$$-\nabla P + \mu\nabla^2\vec{u} + \vec{b} - \rho\frac{d\vec{u}}{dt} = 0 \tag{5}$$

in which $\vec{u}$ is the velocity field, P the pressure, ρ and μ the fluid density and viscosity. $\vec{b}$ represents all body forces that can be neglected. Besides, while assuming a steady-state flow the fluid acceleration is considered zero. Therefore eliminating in equation5 those terms, we can simplify it to,[30]

$$\nabla P = \mu\nabla^2\vec{u} \tag{6}$$

Often in microfluidics, microchannels have a rectangular cross section in which $h \ll w$. In these cases, the channel is so large that it can be approximated to an infinite parallel-plate configuration. For a fluid in mechanical equilibrium, the velocity in the boundaries of the microchannel is considered zero. As illustrated in Figure 1.8, the flow follows the x axis along the channel length (L). Consequently the pressure gradient will depend on the x direction for a constant height.

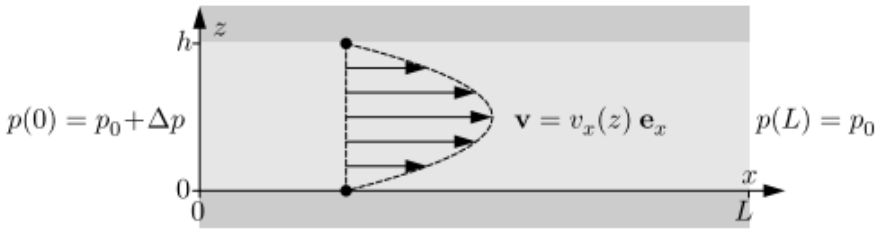

Figure 1.8 Illustration of an infinite parallel-plate channel with height h[22]

The solution can be obtained from equation6, and indicates that the velocity profile is parabolic,

$$v_x(z) = \frac{\Delta p}{2\mu L}(h - z)z \tag{7}$$

The flow rate through a section of width w and height h is obtained by integrating the equation7,

$$Q = \int_0^w dy \int_0^h dz \frac{\Delta p}{2\mu L}(h - z)z = \frac{h^3 w}{12\mu L}\Delta p \tag{8}$$

Following this demonstration is possible to assume that the steady flow allows solving the Navier-Stokes equation for any position of the liquid front,[30]

$$Q(t) = \frac{P(x)}{R(x)} \tag{9}$$

where $R(x)$ corresponds to the hydraulic resistance. Obtaining,

$$R(x) = R_{Hyd} = \frac{12\mu L}{h^3 w} \tag{10}$$

As equation9 demonstrates, the connection between flow rate and pressure within a microchannel where the flow is pressure-driven can be compared with an electrical circuit. By analogy, the volume flow rate corresponds to the electrical current $Q \sim I$, hydraulic resistance behaves similarly to electrical resistance and the fluid pressure corresponds to electrical voltage $\Delta p_s \sim \Delta V$. (Figure 1.9) The hydraulic resistance increases with the progress of the fluid within the channel.[24]

Figure 1.9. Representation of the analogy between microfluidic and electrical circuits[24]

For a pressure-driven flow, the difference of pressure applied is constant and allows the fluid to move within the channel. This pressure can be produced externally to the structure, by a syringe pump connected to the inlet and outlet of the channel. On other hand, in capillary systems, the pressure is generated by the surface of the microchannels, as demonstrated in equation3. For this reason capillary based chips are very attractive for PoC devices.

1.3.5 Capillary pumps

Once the capillary pressure is maintained constant, it is possible to calculate the position of the liquid's interface (meniscus) in function of time. Considering that the microchannel is placed horizontally (Figure 1.10) the capillary flow will keep spreading as long as there is more channel to be wetted. [22]

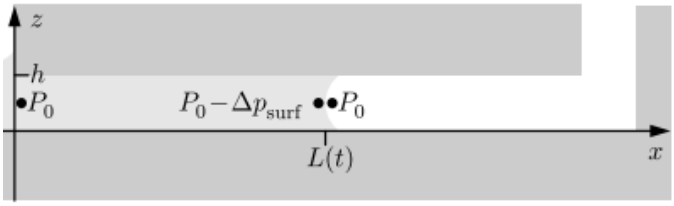

Figure 1.10. Representation of the principle of a capillary pump. $L(t)$ represents the position of the curved meniscus (adapted from [22])

The velocity of the fluid front is determined by mass conservation of the flow in the tube, and can be obtained by[31]

$$v(0,t) = \frac{dL(t)}{dt} \tag{11}$$

For a certain channel is possible to approximate the volume flow rate to the product of the average flow velocity with its cross-sectional-area.[23],[32] Assuming that the position $x = 0$ corresponds to the fluid entrance on the microchannel and a Poiseuille flow profile, at $x = L(t)$ the velocity gives the following relation,

$$v(t) = \frac{Q}{wh} \approx \frac{h^2}{12\mu L(t)}\Delta p \tag{12}$$

Solving the differential equation, the meniscus position in function of time is defined as[22]

$$L(t) = h\sqrt{\frac{\Delta p_s}{6\mu}t} = \sqrt{\frac{\gamma cos\theta h}{3\mu}t} \tag{13}$$

Figure 1.11 shows the existence of a square-root dependence of time for the position of the meniscus within a microchannel [31], as suggested in equation13.

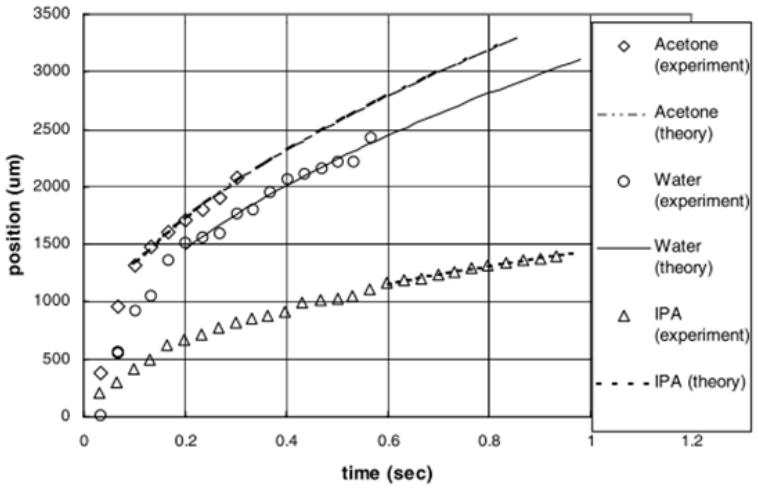

Figure 1.11 Position of a capillary meniscus for different liquids into silicon-nitride microchannel [31]

Autonomous capillary systems are widely used for manipulating fluids for applications such as immunoassays and diagnostic applications. In order for the fluids to flow through the capillary system is necessary to have a pressure source. Therefore in devices with surface tension driven pumping, liquids are pumped passively by capillary effect. This driving pressure depends not only on surface tension but also on the geometry of the surfaces of the microstructure.[33]

As explained previously, the contact angle is a determinant aspect when considering the motion of the fluid. If the microchannel has only hydrophobic surfaces the liquid will be prevented to enter. On other hand, hydrophilic surfaces are able to draw in the liquid by passive capillarity. This way the channel itself will behave like a pump.[33]

Capillary pumps determine the overall flow rate and volume of liquids that can be handled by the device. These structures can have diverse designs that will behave differently while controlling the advancement of the filling front. The simplest design is a microchannel with the adequate volume to accommodate all the liquid. A more complex pump can integrate microstructures, such as posts in the microchannel. In these cases, the posts help to decrease the flow resistance due to the large number of parallel flow paths.[9]

Advanced capillary pumps can also be composed of elongated microstructures that control the filling front by imposing different times for the progression of the liquid along all the directions of the pump. A straight filling is achieved in the microchannel and at the same time the spacing between the microstructures act as pinning sites.[9]

As an example of a capillary pump with elongated microstructures, we can consider two filling strategies, as demonstrated in Figure 1.12. In one strategy the front is guided in alternate directions through several rows (serpentine) and in other the liquid is initially guided to one of the edges of the pump and then fills each row from this point (leading-edge).[34]

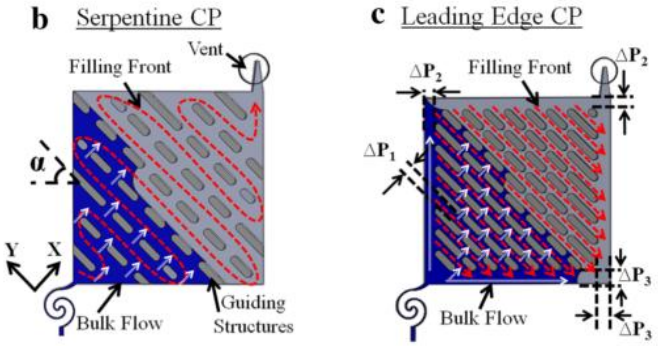

Figure 1.12. Schematics of serpentine and leading-edge capillary pumps[34]

In both cases the filling front flows parallel to the microstructures, spreading along the edge into the next row. Simultaneously the liquid is drawn by the higher capillary pressure into the spacing between parallel rows. The gap between the microstructures acts as a temporary valve preventing

the fluid to pass until the entire row is filled.[34] This filling mode is representative of a capillary pump with a low flow resistance (Figure 1.13).[9]

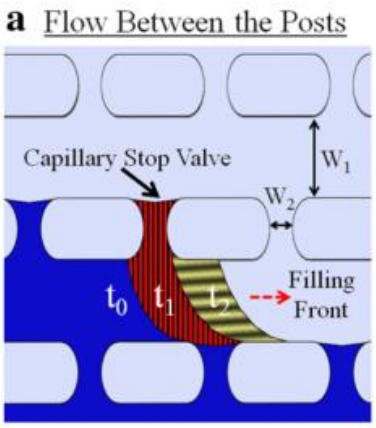

Figure 1.13. Illustration of the progression of the fluid front [34]

These structures introduce a significant improvement when compared with simple microchannels. As mentioned previously, the hydraulic resistance increases while the fluid front advances in the channel. Therefore, the flow rate of a continuous channel tends to decrease with the filling front progression (equation8).

For a microchannel with these microstructures the resistance also increases while the liquid flows through the first row, reaching a maximum when the front reaches the edge. Once the filling front reaches the next row, the two become connected due to the existence of the gaps. These behave like parallel flow paths, and hence the flow resistance decreases as the liquid progresses. However in the overall, as the fluid advances the resistance also tends to increase.[34] As a result in general the flow resistance of a capillary pump with microstructures is lower than of a straight channel.

Biological assays require systems that can comprise solutions used in different steps. This multiple steps can differ not only in volume of solution needed but also in duration. For instances, considering an immunoassay, steps related with the capture of antigens or binding of antibodies require minutes of flowing. Whereas for washing steps the flow can take less time and require a higher a flow rate. Therefore one way of designing a microfluidic system for a specific immunoassay is by connecting capillary pumps with different characteristics that can assure the requirements for each step of the experiment. One important aspect of the connection of pumps is assuring that the first is filled completely before the fluid proceeds to the next one. Thus the control over the filling front is advantageous.[9]

1.4 Capillary microfluidic devices

This sub section focuses on the properties of the materials used for the fabrication of the capillary microfluidic devices. As well a notion of surface treatments that can be performed is included.

1.4.1 PDMS - glass

In the beginning of the development of research in microfluidic devices glass and silicon were the original materials. With the growth of this field a wide variety of materials started to play an important role. Nowadays microfluidic devices can be composed of several materials such as glass, polymers, silicon and metals, depending on the intended application.[17]

The materials chosen have a major importance on dictating the properties of the microfluidic flow path. Microfluidic flow paths combine the geometry and chemical characteristics of materials used to define the structures in which the samples flow from a loading zone throughout the entire device. The flow rate, capillary pressure, wetting, optical properties and adhesion of biomolecules are dependent of the materials used for the fabrication of the devices.[17]

Currently PDMS is the most used polymer for the production of microfluidic flow paths. It belongs to a family of elastomeric polymers that contain silicon oils. These polymers form an elastomer when taken beyond their polymerization temperature and in contact to a reticulating agent.[35] As an elastomeric polymer, PDMS consists on a structure composed of weakly cross-linked chains, characterized for being flexible and elastic after polymerization. This polymer exhibits repeating OSi(CH3)2 monomers, responsible for its hydrophobicity.[12] A reported experiment, defines a water contact angle in a PDMS structure of 109º.[36] Due to being flexible it is easy to form reversible bonds through Van der Waals interactions with other surfaces.[37]

PDMS can be fabricated by soft lithography, where the liquid polymer is mixed with a curing agent and then poured onto a mold. Then the system is placed in an oven at 70ºC in order for the mixture to polymerize and become solid. After solidifying it is peeled off from the mold and the structure has the desired features. The precision of the structures obtained can go the sub micrometric range.[35] An example of a PDMS structure with the channels is illustrated in Figure 1.14.

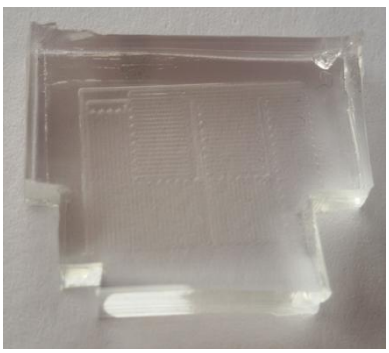

Figure 1.14 Example of a PDMS structure

The widespread use of this polymer is related with the combination of material properties such as biocompatibility due to low toxicity, high electrical resistance, long-term endurance, low elastic modulus and flexible processing techniques.[38] However the use of this polymer shows some drawbacks like the possibility of nonspecific adsorption and permeation by hydrophobic molecules, and poor wettability with aqueous solutions.[6],[12] Besides, the properties of the reticulated polymer don't show long term stability.[35]

As mentioned previously, autonomous movement of fluids in a hydrophilic microchannel is dominated by surface tension. However if considering a channel composed of a hydrophobic material, surface tension alone is not capable of inducing a fluid flow.[29] One way of addressing this challenge is to bond the hydrophobic structure to a hydrophilic material.

Glass is characterized by a contact angle between 0 and 30º depending on the surface treatment (that will be addressed in section 1.4.2).[24] Glass substrates are also optically transparent and not electric conductive. These properties make this material good for performing immunoassays through microfluidic devices.[12]

Regarding the use of these materials, for a device composed of PDMS channels sealed with a glass slide, equation3 can be simplified to,

$$\Delta p_s = \gamma \left(\frac{cos\theta_{glass} + cos\theta_{PDMS}}{d} + \frac{2cos\theta_{PDMS}}{w} \right) \quad (14)$$

As equation14 suggests the wettable wall has a major impact in generating a positive capillary pressure to force the fluid motion within the channel. Therefore glass, that has a highly hydrophilic surface, can be chosen as the "motor" of the capillarity of this device.[25] The geometry of the device also influences the capillary pressure, in a way that for smaller channels the pressure obatined is higher.

Hybrid microfluidic devices like PDMS-glass have gained more attention, due to the combination of the advantages attributed to each of the materials. In this case, the devices combine characteristics like fast fabrication, flexibility and biocompatibility.[12]

1.4.2 Surface treatment

In capillary microfluidics, surfaces play a determinant role since they define properties like wetting, adsorption of biomolecules, sealing and bonding to different materials.[39] In order to achieve a functional PDMS-glass sealed microfluidic device it is essential to have both surfaces in contact, cleaned. Therefore the fabrication of these devices should include a surface treatment step.

Surface treatment processes can be divided in two main groups: wet and gas phase treatments. In the first case it depends on the action of reagents capable of altering surface properties, such as coatings and detergents. On other hand, gas phase treatments not only can modify surface chemistry but also can affect its roughness.[17]

Wet and UV/Ozone cleaning techniques are used to eliminate organic contaminants.[40] In order to achieve an effective level of cleanliness it is required to perform a step of wet cleaning before the UV/Ozone treatment. This preliminary step is carried out to remove contaminants like dust and salts that cannot be converted into volatile products.[41] Figure 1.15 represents the effect of combining both techniques.

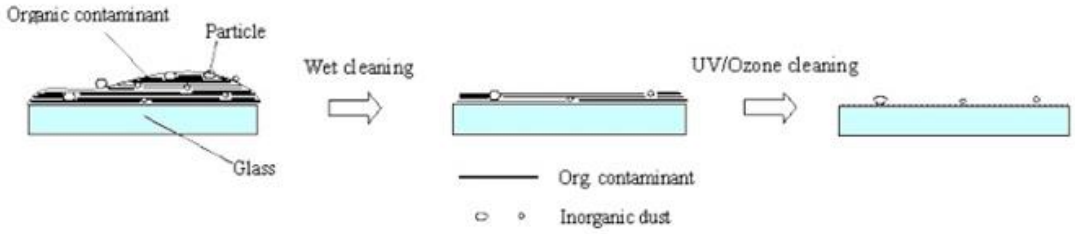

Figure 1.15 Illustration of the UV/Ozone cleaning process [40]

UV/Ozone cleaning relies on the use of a low pressure mercury lamp that emits radiation in two different wavelengths. The most energetic radiation (184.9nm) allows for the transformation of oxygen in ozone, and the other (253.7nm) reacts with the created ozone to oxidize hydrocarbon contaminants at the glass surface. This method is quite effective in removing organic contamination with thickness in order of one monolayer, without sample surface contraction and overheating. One consequence of using this technique for cleaning glass substrates is the transformation of these surfaces into hydrophilic and highly wettable.[41]

Surface tension and contact angle of a material depend on the formation of organic compounds. When the surface is contaminated the surface tension decreases and the contact angle is wider. According with the different methods of action, both cleaning techniques induce a different response in the surfaces that can be measured through the contact angle of a water drop. The water contact angles associated with the combination of both techniques, only wet cleaning with detergent and water and without treatment are 4º, 13º and 25º respectively.[40] (As illustrated in Figure 1.16)

Figure 1.16. Spreading effect of a water droplet in glasses cleaned with a combination of wet cleaning method and UV/Ozone (a), only wet cleaning (b) and unprocessed (c), respectively [40]

After cleaning the glass surfaces present a high surface energy. Thus they have a huge tendency to adsorb particulate and organic contaminants from the involving environment. For this reason is recommended to use the substrate within few minutes after the cleaning process.[41]

1.4.3 Sealing

When developing microfluidic devices several challenges such as confinement of solvents, samples and reagents in defined volumes; prevent spreading of liquids among undesirable areas; reduction of contamination and prevention of evaporation and protection of samples, come into play. Towards addressing these issues is fundamental to analyze properly the sealing conditions of the device.[42]

Several bonding methods are available depending on the materials that compose the device and its application. Sealing techniques can be divided in two categories, irreversible and reversible. Devices with irreversible sealing of the constituting layers are associated with a high strength bond and thus permanent. While performing this method it is essential to include a step of surface treatment in the fabrication, by exposing both surfaces to oxygen-plasma or UV/Ozone treatment.[43] Whereas reversible bonding exists due to weak bonding that can be disassembled if necessary.[44]

Reversible bonding can be performed through self-adhesive property of the materials and used to seal polymers with hard materials such as glass and silicon, with or without surface modification. However this method presents potential for leakage problems that can be managed through the choice of the materials and the control of working pressures and flow rates of the structures.[44]

PDMS is widely used in microfluidics and has the advantage of allowing reversible van der Waals interactions with other surfaces. This bonding is possible due to the attraction between molecules and surfaces.[44] Therefore a PDMS structure sealed with glass can be obtained by putting in contact both structures surfaces (as shown in Figure 1.17). In order to avoid the incorporation of dust particles or bubbles both surfaces need to be carefully checked and if necessary cleaned. In case it happens, it is possible to peel off the PDMS from the glass, clean it and repeat the sealing.

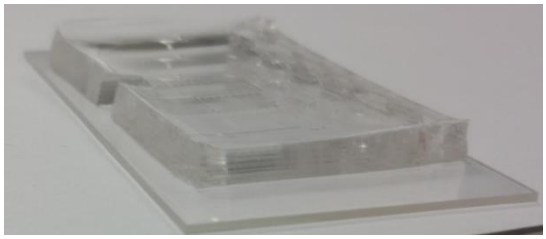

Figure 1.17 Example of a PDMS-glass microfluidic device

1.5 Immunoassays in capillary microfluidic systems

Immunoassays are widely used for the detection of antigens. There is a variety of formats that will define the complexity of the devices where they are performed. Performing immunoassays in microfluidic systems introduces numerous benefits, for instances, reduction of assay time, consumption of reagents and enhancing reaction efficiency. While most immunoassays require several steps such as washing, mixing and incubations that are laborious and time consuming.

Besides, immunoagents needed to perform immunoassays can be very expensive. One advantage of the miniaturization of the assays is the decrease consumption of these species.[12]

In all cases the sensitivity and specificity of the antibody-antigen interaction allows for the quantification of small molecules.[12] Signal detection is essential and can be achieved by using reactive species that can quantify a certain analyte.

In fact Enzyme Linked Immunosorbent Assay (ELISA) is a very common diagnostic tool. The demand is related with their high specificity, sensitivity and versatility in allowing the detection of different types of analytes. This technique starts with the coating of an antibody in a substrate, to which a sample is applied. If any of the target antigens are present in the solution, the binding to the antibodies immobilized is detected by a readout method.[45]

Microfluidic immunoassays can be divided in several categories. The first set of categories relates with whether it depends in immobilization of probes in a substrate. In this case there are two types of assays: homogeneous or heterogeneous. In homogeneous assays both probes and sample are mixed in liquid phase, which requires a separation step in order to be able to detect the reaction products.[45] These assays benefit from multiplexing and fast electrophoretic separation, though they require pre-concentration steps.[12] On other hand, in heterogeneous assays the probes are immobilized in the substrate surface where the complex forms.[45] The latter has the advantages of allowing an easy wash away of particles that did not bound to the probes, high surface area/volume ratio and good sensitivity. However heterogeneous methods require extra steps for immobilizing the probes.[12]

Immunoassays can also be divided into three more categories, depending on the interaction between the different species: competitive, indirect and sandwich. A competitive ELISA is based in a competitive binding process between the sample antigen and an add-in antigen. The protocol for a competitive assay requires a solution with antibody-antigen complexes and free antibodies to be mixed with antigens immobilized in a surface. After washing, only the free antibodies linked to the antigens remain. Then, a second antibody with affinity to the primary antibody and labeled with, e.g. Horseradish peroxidase (HRP), is added. In order to obtain signal 3,3',5,5'-tetramethylbenzidine (TMB) or luminol can be introduced. The competition happens between the antigens within the incubation solution and the antigens immobilized in the well.[46] (As illustrated in Figure 1.18).

Another classification introduces indirect immunoassays. In this type of assay there is also an incubation step in order to form antibody-antigen complexes, but this time the antigens are attached to the surface of the well. Then the antibodies that didn't link to the antigens are washed away. After that a secondary labeled antibody is introduced in the solution, allowing for the binding of antibodies and signal reading.[46] (Figure 1.18)

Some of the advantages of performing a competitive ELISA is that it has high specificity and flexibility, allowing the combination with an indirect method, creating an indirect competitive ELISA (icELISA).[47] The principle behind this icELISA is that the antigen present in the sample has to

compete with those immobilized on a surface for the binding to the antibody in solution. Thus, the signal detected is inversely proportional to the amount of antigens used to form the antibody-antigen complexes.[46,48]

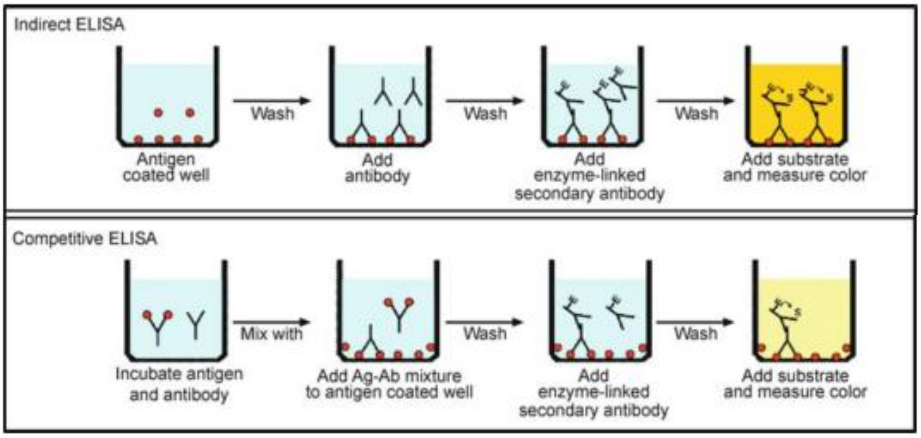

Figure 1.18 Schematics of the protocols for an indirect and competitive ELISA [46]

One way of simplifying the immunoassays described is by labeling the primary antibody. This way eliminating the need for a second labeled antibody, not only the signal detected will be the same but also the resources used to perform the assay will decrease.

The final step to consider when performing an immunoassay is the signal detection. Depending in the tags used to label molecules, the most common detection techniques that can be used are chemiluminescence, fluorescence and colorimetry. The latter presents a significant interest for PoC applications since is compatible with a simple setup and an easy detection.

Colorimetric detection is obtained through the catalyzation of TMB by the enzyme HRP that leads to the production of a colored precipitate. The precipitate causes a color change of the substrate that can be monitored.[46] The signal detected is proportional to the amount of antibodies labeled with the enzyme that are able to link with the antigens in the surface.

1.5.1 OTA immunoassay

Ochratoxin A (OTA) is a mycotoxin known as nephrotoxic, immunotoxic and carcinogenic for animals, produced by toxigenic species of *Aspergillus* and *Penicillium*.[49] OTA is involved in contamination of a variety of food (wine, beer and coffee) and feed at a global scale.[50] Due to its chemical stability against heat and during food processing it is considered one of the most abundant food contaminating mycotoxins.[49] European Union regulation has restricted limits to the concentration of this toxin in commercialized products.[51]

Due to all the harmful effects related with this toxin, methods for the detection and quantification have been studied for a long time. Thus, devices capable of presenting *on site* quantification are

becoming more attractive. Microfluidic devices are therefore a good platform, since they are not very time and reagent consuming.[26]

Several strategies based on competitive immunoassays have been used or the detection of OTA.[50] This thesis proposes an approach based on icELISA in a capillary microfluidic chip.

The assay is performed by first immobilizing in the channel control OTA molecules, for instances, the OTA-BSA conjugate. The simplest form of immobilization is based on physical adsportion of probes onto the surface.[52] Then the anti-OTA is diluted in the sample that also contains known concentrations of OTA. Thus the anti-OTA will be able to bind to the OTA molecules in solution or to the OTA-BSA conjugate in the surface.[26]

While performing immunoassays it is essential to eliminate all sources of false positive results. One main source of these results is non-specific adsorption of molecules in the surface of the channels. This problem can be avoided by coating the surface with proteins, like bovine serum albumin (BSA). BSA is a protein with high solubility with a tendency to link to hydrophobic substrates, such as PDMS.[45]

Often, samples are prepared and pretreated before being analyzed. Changes on the biological activity of a sample can happen due to the interaction with other species. One way of preserving its properties is by buffering the sample. Phosphate buffered saline (PBS) is one of the most common buffers, owing to having a pH near 7.4. It is frequently used in dilutions, and particularly when a sample is spiked with known concentration of a specific analyte.[39]

In this icELISA the competition occurs between the OTA molecules in solution and the OTA present in the immobilized conjugates. As a result, an increase in the concentration of OTA free molecules in the solution will induce a decrease in the signal, since fewer antibodies connect with the immobilized species.[26]

2 METHODS

This chapter describes the several microfabrication techniques that were used to fabricate the capillary biochip. The preparation of the biological experiments to test the device is also described.

As explained previously the capillary chip is a structure composed of PDMS and glass. The production of this structure comprises several steps, including the fabrication of a hard mask, SU-8 mold and finally the PDMS. The sub-section 2.1 focuses on the several techniques used to create the chip. In sub-section 2.2 the working principle of the capillary microfluidic and the evolution of the chip design, considering the application proposed. In the last sub-section 2.3, all the preparation relative to the biological experiments is explained, including the protocol of the OTA immunoassay and a brief explanation about data analysis.

2.1 Microfluidic devices fabrication

2.1.1 Hard Mask design and fabrication

The first step to create the desired structure is the mask design (as illustrated in Figure 2.1). AUTOCAD is the software used for this purpose. After creating the drawing, it is necessary to transfer it to an Aluminum substrate that will be used to create the hard mask.

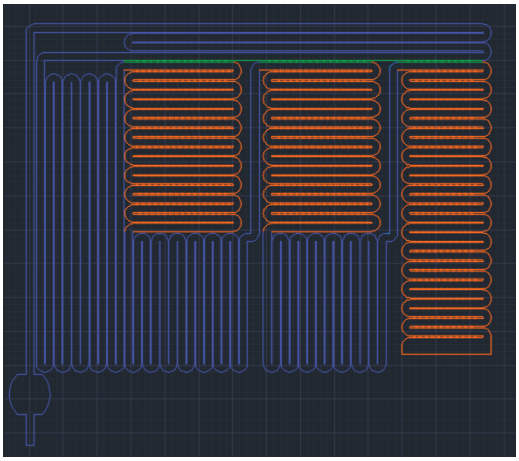

Figure 2.1 Representation of the AUTOCAD design

Within the production of the chip, several steps depend on the use of a clean glass slide. Therefore, this cleaning step is one of the most important processes, and has to be handled carefully. In order to be sure that the whole surface of the slide is properly washed, it is firstly rinsed with abundant acetone and water. After that the slide is immersed in a detergent solution (Alconox) and placed in a water bath at 65ºC, for 20 min. Alconox is a concentrated anionic detergent usually used for cleaning laboratory glassware from contaminants.[53] Following the bath, Alconox residues must be removed, therefore the glass slide is once again rinsed with abundant water. At last the slide is dried with compressed air.

Most of the following processes take place in a class 100 clean room area, whereas lithography is performed in a class 10 clean room. The deposition of Aluminum into the glass slide is performed in Nordiko 7000 (sputtering). After depositing a 2000 Å thick Al film is obtained.[54]

The exposure of the substrate to the laser that will do the patterning is preceded and followed, respectively by a coating and development step. Both steps occur in a line-track (by SVG). The spin coated photoresist is 1.5µm thick (positive resist). Optical lithography is performed with a direct write laser (DWL by a 442nm Helium-Cadmium laser) that scans the surface and allows for the patterning of the AUTOCAD design.[54] Since the photoresist is positive, during the development the exposed areas will be dissolved (as illustrated in Figure 2.2).

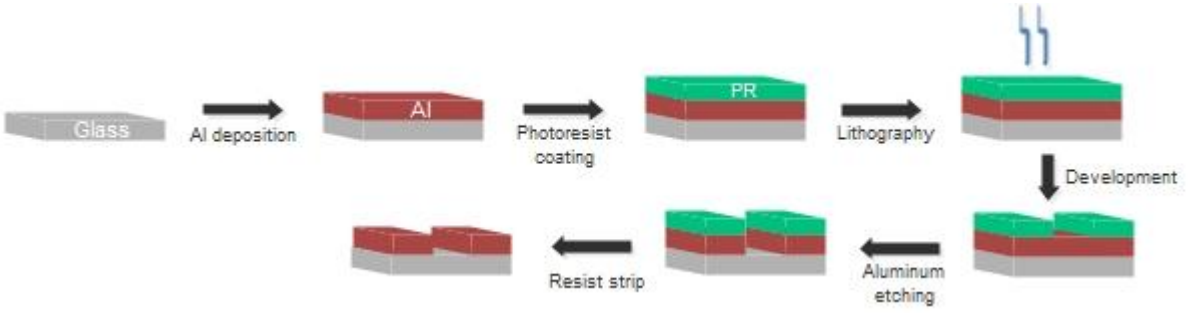

Figure 2.2 Hard mask fabrication

Once the development is complete, Al has to be removed from the unexposed areas. This is accomplished by wet etching the sample with an aluminum etchant (Aluminum Gravure Etchant from Technic), followed by rinsing with abundant water. The final procedure of the hard mask fabrication is to remove all the photoresist residues. This is obtained by washing the sample with acetone and water. In the end the sample is dried with compressed air and checked in the microscope to verify if everything was well patterned and removed. Figure 2.3 shows a microscopic view of details of two different sections of the mask. Figure 2.4 shows the final aspect of the hard mask.

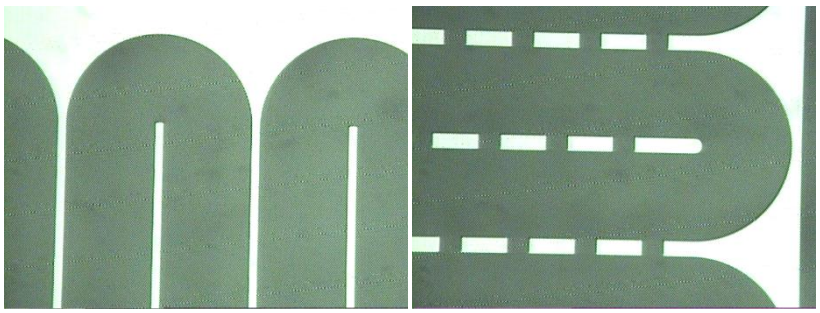

Figure 2.3 Hard mask details after aluminum etching and resist strip

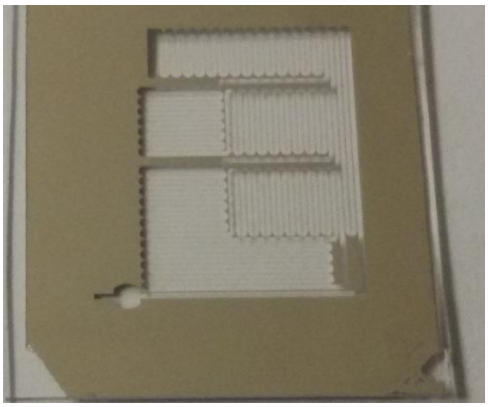

Figure 2.4 Hard mask

2.1.2 SU-8 mold

Afterwards the production of the hard mask, the proceeding step is the fabrication of the SU-8 mold. This mold is the starting point for manufacturing the PDMS structure with the desired features. In order to avoid contaminations this process takes place in a laminar flow hood.

The SU-8 (photoresist) is spin coated in a Si substrate. Before pouring the SU-8, the Si substrate is cleaned (the cleaning protocol is similar to the one described for glass slides in section 2.1.1). The Si substrate is rinsed with acetone and IPA and then immersed in an Alconox solution and placed in water bath at 65ºC, for 20 min. Once again, after the bath the substrate is washed with abundant water and dried with compressed air. Additionally to the wet treatment, before the spin coating, there's also a step of UV/Ozone treatment of the surface (for 25min) in order to help the spreading of U-8.[55]

Depending on the desired height there are several formulations of the photoresist that can be used. In this work, it was used SU-8 50 (Microchem) in order to fabricate channels with 50µm in height. According to the manufacturer recommendations, a normal process should comprise the steps: coat, soft bake, exposure, post exposure bake, development and hard bake (as demonstrated in Figure 2.5).[56],[55]

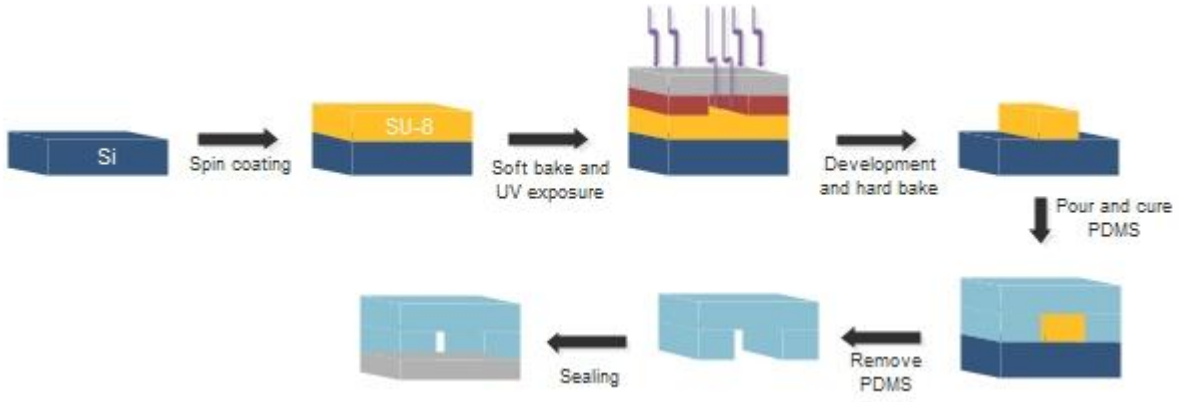

Figure 2.5 SU-8 mold and PDMS fabrication

SU-8 is poured on the Si substrate and spin coated (Laurell WS-650MZ-23NPP/LITE automatic spinner). The appropriate spinning conditions must be chosen depending on the desired thickness. In this work, the spinning protocol comprises 2 steps. These steps correspond respectively, to the spread cycle (that allows the resist to spread in the surface) and the spin cycle (Table 2.1).[56]

Table 2.1 Spinner parameters for coating of SU-8 50[56]

	Velocity (rpm)	Acceleration (rpm/s)	Spinning time (s)
Step 1	500	100	10
Step 2	2300	300	37

After spinning the resist, the sample is placed in a hot plate. This bake step allows for the evaporation of the solvent and to help solidify the film, and can be divided in a pre bake at 65ºC, for 3 min and soft bake at 95ºC, for 8 min. The progressive heating, starting at lower temperatures enables a more controlled evaporation allowing for a better coating.[56]

Once the bake is finished, the hard mask is placed on top of the sample, with the Al facing down, in contact with the SU-8. The set is then exposed to a UV source for 25s, in order to transfer the pattern from the hard mask to the SU-8. After the exposure the sample is submitted to a second baking step, the post exposure bake. Once again the bake is divided in 2 phases, at 65 ºC for 1 min and 95ºC for 7 min, respectively. Since SU-8 is a negative resist, the exposure to UV enables the cross-linkage of the areas exposed. The changing of the properties of these areas allows them to become non-soluble. Therefore, upon development by immersion in PGMEA the unexposed areas are dissolved.[55]

Finally the sample is rinsed with IPA, dried and submitted to a hard bake at 150ºC for 15min (Figure 2.6 shows a SU-8 mold after fabrication). The profile of the channels on the SU-8 mold can be verified using a microscope and profilometer.

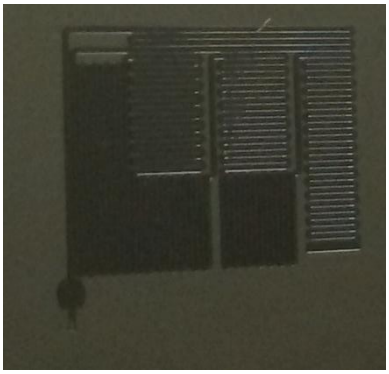

Figure 2.6 SU-8 mold

The microscope inspection is a critical check point for the fabrication. Because, the mold might seem to be in good conditions, but when verified some of the channel walls can be poorly defined. Problems in definition of the channels can be traduced in bad definition of the PDMS walls and channels and therefore affecting the dimensions, the capillary structure performance is also affected. This step was performed in a Leica DLML microscope. Figure 2.7 shows two examples of molds were the walls are not well defined (A and B), in contrast with two mold in perfect conditions (C and D). As can be observed the problems lie on the fact that in the top pictures it is not possible to see the end of the walls, whereas in the bottom one can see that the exposure got through all the depth of the SU-8.

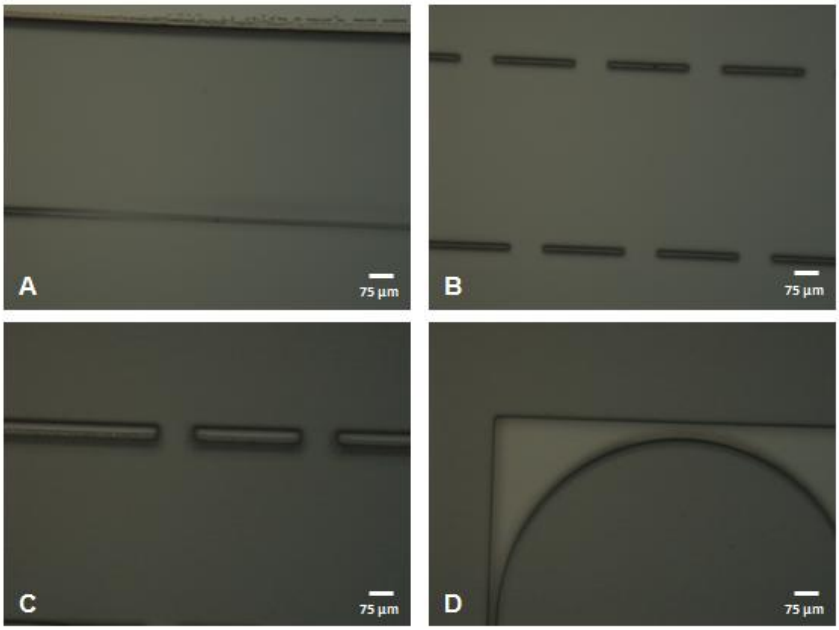

Figure 2.7 Microscope inspection of the SU-8 mold after fabrication (Leica 10x). Pictures A and B represent molds not well defined and pictures C and D exemplify the result of a good fabrication

2.1.3 PDMS- glass microfluidic device

The SU-8 mold is used to define the designed structure in PDMS. PDMS is obtained by mixing a curing agent with a liquid polymer base, both in liquid form at room temperature, in a ratio by weight of 1:10 (Sylgard 184, Dow Corning). While mixing both compounds several bubbles appear, hence is necessary to degas the mixture in vacuum for about 30 min. After all the air bubbles are removed, the PDMS is poured onto a petri dish that contains the SU-8 mold and cured for 1:30h at 70ºC.[37]

Once the PDMS is cured, it is removed carefully from the mold, to avoid damage. With this method the SU-8 can be used repeatedly for replica molding.[37]

As referred before, if the SU-8 mold has any imperfection, those will be imprinted in the PDMS structure. Figure 2.8 compares two structures where the channel walls are not well defined (A and B)

with two that allow the correct fluid motion (C and D). One consequence of the problems in the channel walls is that the fluid can leak and not follow the right path.

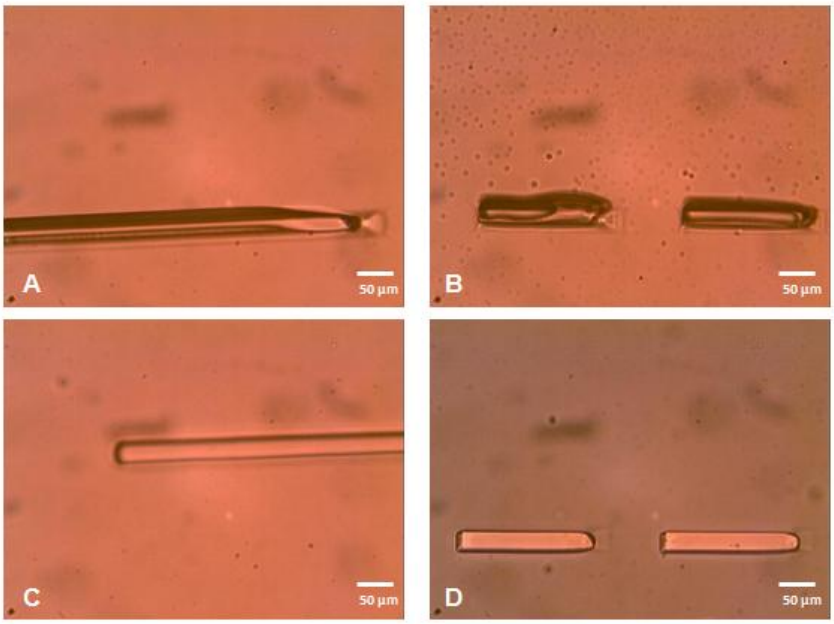

Figure 2.8 Microscope inspection of the PDMS structure (Amscope 20x). Pictures A and B represent channels not well defined and pictures C and D illustrate functioning channels

In order to be able to use the PDMS it is necessary to seal the structure onto a cleaned glass slide (as shown in Figure 2.9). Prior to mounting the PDMS-glass set, the glass surface is cleaned as described previously with an additional UV/Ozone treatment for 6min (UVO Cleaner 144AX-220, Jelight Company). The UV/Ozone treatment takes 6minutes with extra 5minutes for exhaust of the ozone produced. The relevance of this treatment is the oxidization of the surface to control its hydrophilic characteristics. Since considering a reversible bonding, both surfaces are bonded by pressing together manually the structures. It is essential to make sure that there are no air bubbles or dust particles trapped between the surfaces. In case that happens the structures can be separated, re-cleaned and re-bonded.[37]

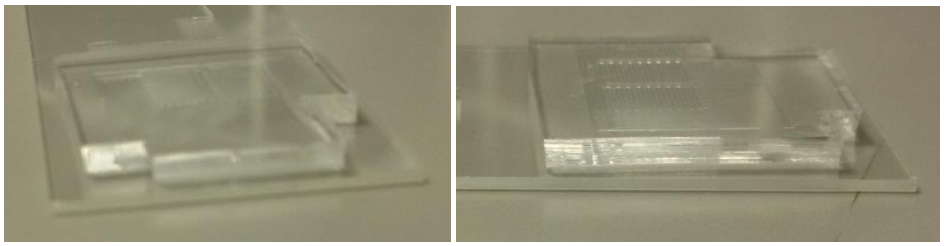

Figure 2.9 PDMS-glass microfluidic device

2.2 Capillary device

As mentioned before, the aim of this work was to design, test and optimize a microfluidic device that capable of handling solutions through capillarity. Therefore the device needed to address several requirements, namely, no need for external pumps, channels capable of handling different flow rates and volumes and signal detection through colorimetry.

In order to obtain a capillary device that could respect all the necessities, several versions were tested. This subsection focuses on the designs used and explains what were the main concerns that led to changes between them. The working principle of both pumps is also mentioned.

It is important to refer that the design of the pumps was based on a previous work developed on INESC-MN.[26]

2.2.1 Working principle

In section 1.3.5 the filling mode of two different channels is explained. As mentioned before, several architectures can be considered for the pumps. The simplest model consists on a continuous microchannel. In this case, the fluid flows through the channel (as shown in Figure 2.10) with a resultant decrease on velocity. This decline results on the accumulation of hydraulic resistance. To this channel we refer to as *slow* pump.

A slow velocity is important in steps for adsorption of molecules in the channel, or binding of antibodies and antigens. Therefore in these cases a *slow* pump is more adequate. The spacing between microchannels that compose the *slow* pump is 25µm.

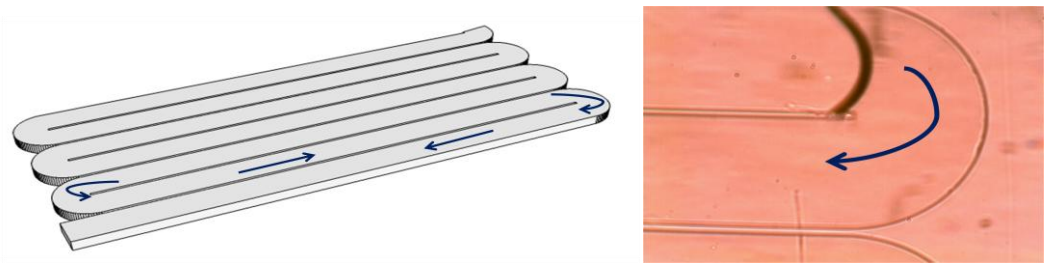

Figure 2.10 Illustration of the fluid flow through a *slow* pump: (left) schematic view in 3D and (right) microscopic view (Amscope 10x)

However, if considering a structure with only slow pumps, the velocity will reach significantly low values and the flow can stop. Therefore the need of creating pumps that assure a greater velocity arises. These pumps are called *fast pumps* and integrate posts within the microchannels walls. The posts create *passageways* that allow for the fluid to pass. For this pumps, the spacing chosen between microchannels is 50µm, resulting in passageways with dimensions of 50x75µm^2.

As illustrated in Figure 2.11 the filling process occurs in two directions. For the bulk flow, there is a straight filling through the main channels in a parallel and alternate direction. Simultaneously the

liquid is drawn to the spacing between the posts. When the liquid front reaches the following channel, the liquid in the valves is adjoined. Consequently the flow velocity is higher than in a *slow* pump.

Fast pumps are adequate to washing steps in which is important to maintain a high velocity to remove the non bonded species. However, in the overall the velocity of the system tends to decrease.

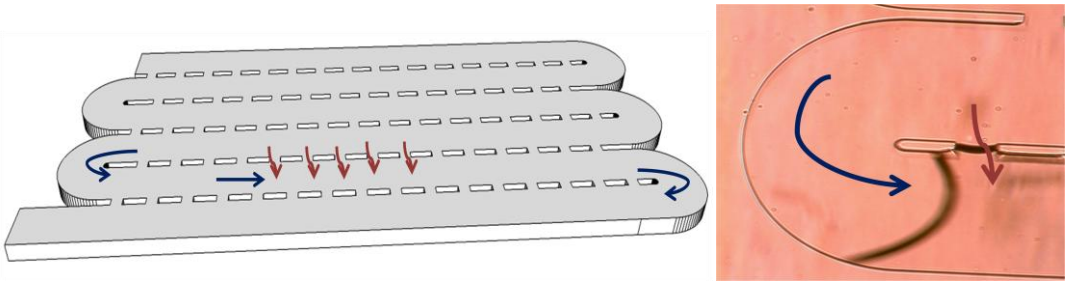

Figure 2.11 Illustration of the fluid flow through a *fast* pump: (left) schematic view in 3D and (right) microscopic view (Amscope 10x)

Let us consider now the effect of placing a *slow* pump followed by a *fast*. As illustrated in Figure 2.12, the velocity of the straight channels tends to decrease with the accumulation of hydraulic resistance. Once the fluid advances to the *fast* the effect of the passageways induces an abrupt increase in fluid velocity.[26] This figure allows to understand the effect in velocity curves of designing a capillary device as a sequence of *slow* and *fast* pumps.

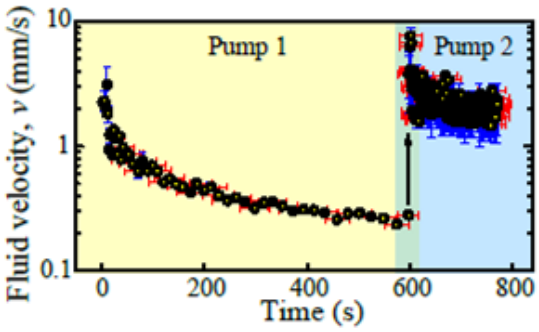

Figure 2.12 Fluid velocity for a slow pump followed by a *fast* pump[26]

2.2.2 Evolution of the capillary device

One main issue to consider when designing the structure is the sequence of the pumps. This is due to the fact that in a device developed for a specific immunoassay, it is essential to assure the right flow conditions for each solution.

Another important requirement is to introduce a specific region of the structure where the resultant signal could be read. Therefore all structures begin with a larger chamber, called *reaction chamber*,

represented in Figure 2.13. Throughout all the versions the channels dimensions are 50μm and 300μm of height and width, respectively.

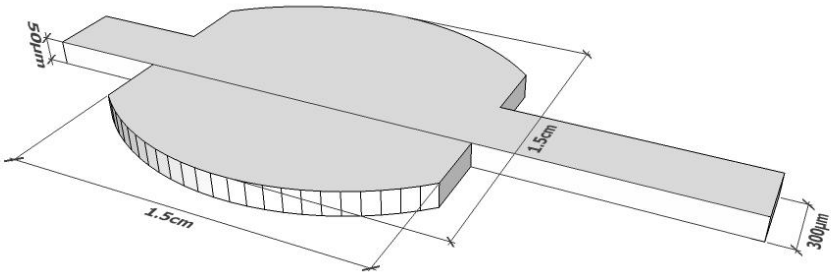

Figure 2.13 Details of the reaction chamber

In order to understand the real behavior of the pumps, several versions were fabricated with various modifications between them. Version1 was designed with the purpose of studying the effect of the length of the channels in the velocity and position of the meniscus and also the effect of intercalating *slow* and *fast* pumps. Therefore in this design (Figure 2.14) the fluid begins to flow in a *slow* pump, then passes through a *fast*, again a *slow* and ends in a *fast*. For this structure, the spacing chosen between channels was 10μm. However during the fabrication several problems aroused in the definition of the channel walls. In order to solve this problem, for the following structures it was defined a spacing of 25μm.

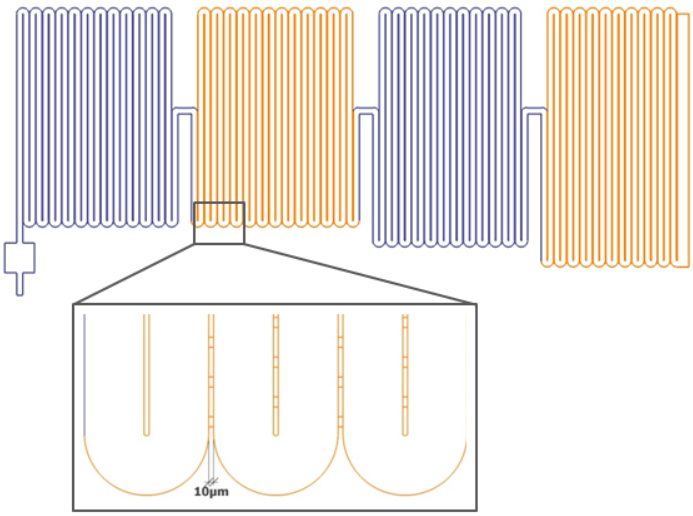

Figure 2.14 Illustration of the device's version1

An additional modification performed was the shape of the reaction chamber. Within the rectangular format, the fluid was not able to fill the corners of the chamber. Towards solving the problem of non-homogeneity of the solution in the chamber the borders were changed to an oval shape (as shown in Figure 2.15). While testing version1, it was noticed that the length of the pumps was exaggerated,

leading to a very small velocity. Therefore, and being unsustainable to have a device that took more than 1h to fill, the size of the pumps was changed, leading to the design of version2.

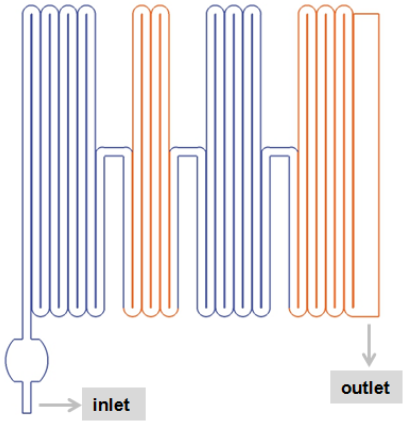

Figure 2.15 Illustration of the device's version2

In version3 was also introduced a set of passageways between the first slow pump and the following fast pumps. These passageways establish a shortcut that allows for the liquid to pass, with a significant decrease in resistance. (Figure 2.16)

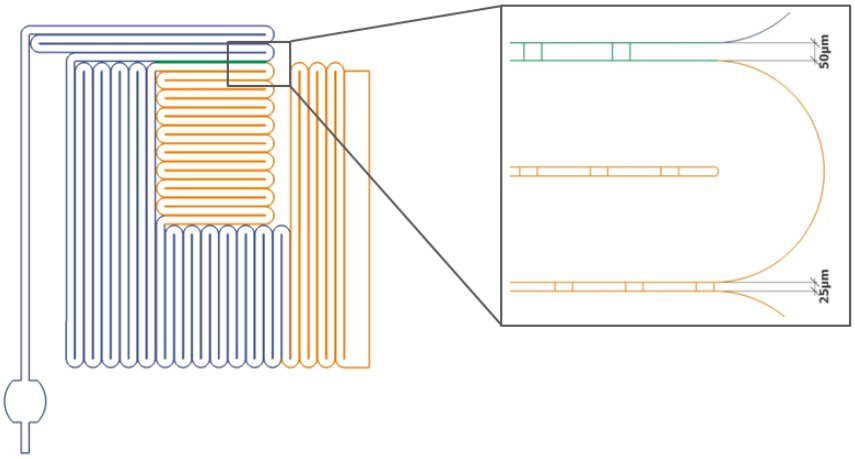

Figure 2.16 Illustration of version 3 with details of the different spacing between channels

Between versions 4 and 5 the only difference is the incorporation of two more pumps. This modification was needed to assure the device's capacity to pull all the solutions for the realization of the immunoassay. (Described in section 2.3.2)

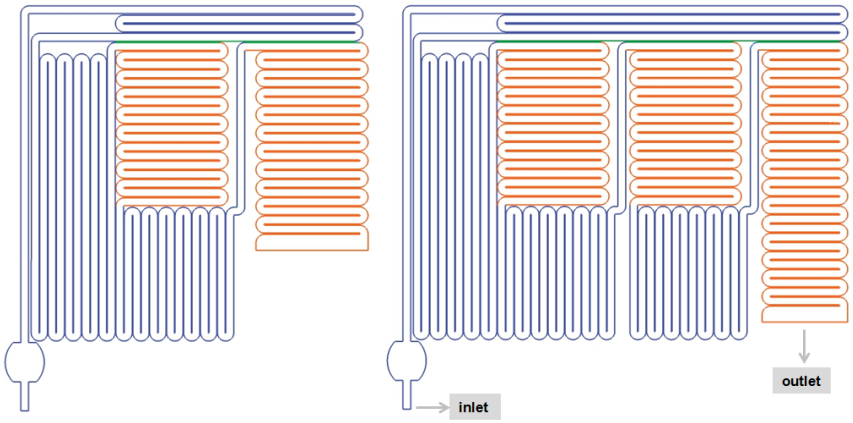

Figure 2.17 Illustration of version 4 (left) and version 5 (right)

The last version (Figure 2.18) designed was based in version5 with the inclusion of an initial module for sequential introduction of the solutions (based on a previous work developed in INESC-MN [13]) The number of inlets varies with the assay steps, in this case the module is composed of 6 inlets. Each one of the inlets is in contact with a common microchannel via passageways of 50x50μm^2. Besides, each inlet is also in contact with the previous one through a 40μm wide channel that acts as a valve.

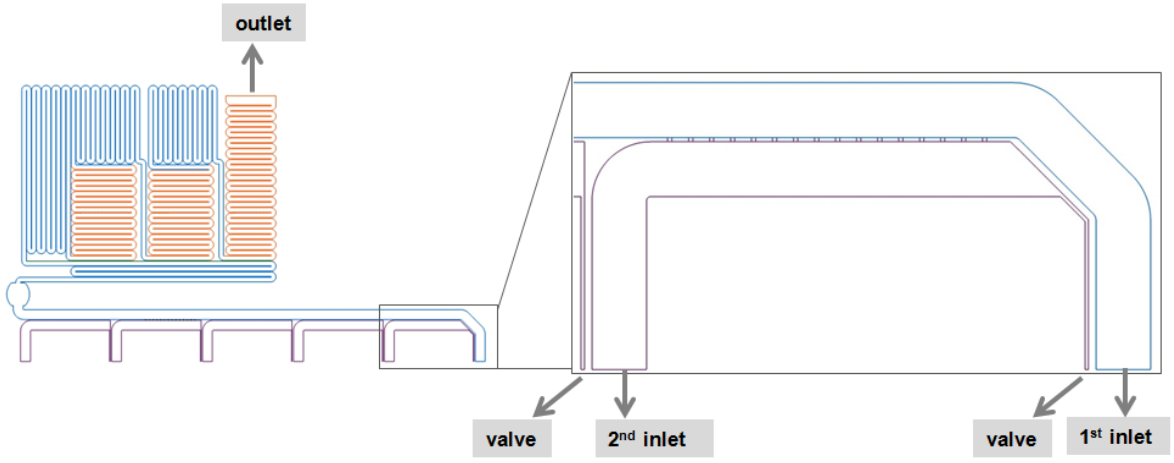

Figure 2.18 Illustration of version 6 with details for the sequential inlet module

The working principle of the module is similar to the one of the fast pumps. In the beginning all the solutions are placed at the entrance of the inlets. The liquid enters the 1st inlet and flows through the common microchannel. While the 1st liquid is flowing the valve is covered, preventing the next solution to flow into the structure. Once all this liquid is consumed, the valve is open to air, inducing the entrance of the next liquid in the next inlet, and successively. (As represented in Figure 2.19)

The existence of the passageways allow for all the solutions, except the initial one, to enter the common microchannel. As for the previously explained fast pump, these passageways also behave as valves that prevent fluid progression, until they get in contact with the next solution.

Figure 2.19 Illustration of the fluid flow through the 1st and 2nd inlets of the sequential module

2.3 Biological experiments

2.3.1 Solution preparation

OTA[57], PBS and OTA-BSA conjugate[58] were purchase from Sigma-Aldrich. Ochratoxin A Antibody-HRP was purchased from ImmuneChem[59] and TMB from ThermoFisher Scientific.[60]

The solutions were prepared by diluting the stock in PBS. The surface blocking agent, a 4% (w/w) BSA solution in PBS was prepared from a Sigma-Aldrich A7906 stock. The BSA solution was stored in the fridge at 5ºC and used in several experiments. The OTA-BSA solution used was from a 1mg/mL stock. Whereas anti-OTA HRP and OTA were diluted in PBS (Table 2.2).

Table 2.2 Preparation of the diluted solutions of OTA and Anti-OTA HRP

Solution	Stock concentration (µg/mL)	Final concentration (µg/mL)
OTA	100	1
Anti-OTA HRP	250	5

Four assays based on different OTA contamination levels of the anti-OTA HRP solution were performed. Therefore 4 samples of anti-OTA HRP with 0, 1, 10 and 100ng/mL of OTA were prepared.

2.3.2 Capillary icELISA

As mentioned in the previous section, the device was designed in order to incorporate the OTA immunoassay. Therefore every pump has a specific purpose. In order to exemplify the explanation, let's consider the following denomination for the pumps (Figure 2.20). In this structure, the fluid begins to flow through the reaction chamber, then goes to the *slow1*, *fast1*, *slow2*, *fast2*, *slow3* and to the last pump, *fast3*. The volumes of the solutions introduced are equivalent to the volume of the pumps. That way and considering the design correspondent to version 5, the volumes supported by the pumps are 3, 1.2, 1.3, 1.2, 1.3 and 1.5 µL, respectively.

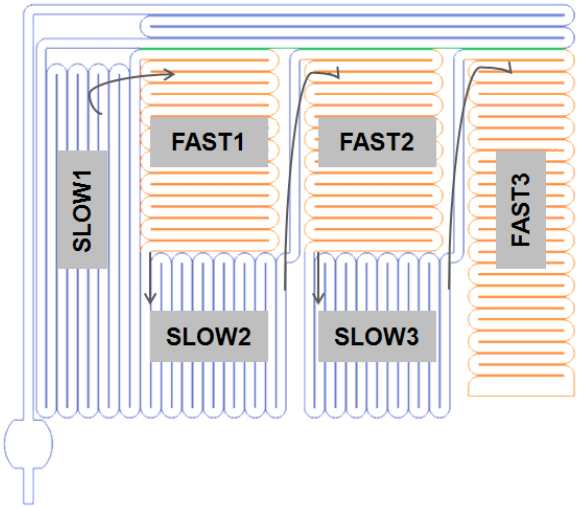

Figure 2.20 Pumps identification according to the order of the fluid flow

This icELISA comprises 6 steps. The first step is to immobilize the OTA-BSA conjugate in the surface of the channel. The immobilization is carried out by spotting with a pipette 0.4µL of the stock solution in the reaction chamber area. This process is performed in the PDMS, before the structure is sealed with the glass slide. It is essential to make sure that the droplet evaporates before the sealing, otherwise the remaining liquid will affect the capillarity of the system and it is not possible to realize the assay. In order to avoid dust and particles contamination, the spotting step was performed in a laminar flow hood. The controlled environment of the hood also helps with the evaporation.

The glass slide used to seal the device is previously cleaned and exposed to the UV/Ozone treatment for 6minutes. Once the treatment finishes the glass is put in contact with the PDMS that already has the spotted OTA-BSA conjugate. The immunoassay starts 5-10minutes past the exposure treatment.

After spotting the OTA-BSA, the surface needs to be blocked in order to avoid non-specific adsorption. As mentioned before the blocking agent used is BSA (*slow1*). It is important to point out that BSA is a viscous solution, thus it creates obstacles while flowing in capillary systems. Consequently, one way of avoiding this problem is by introducing a small volume of PBS before BSA, so that a less viscous front is responsible for pulling the solutions.

Once the blocking is done, the remaining and not immobilized molecules have to be washed away. The washing step is executed by PBS. Since it requires a higher flow rate, this process is associated with the fast pumps (*fast1* and *fast2*). After washing, the following solution introduced is anti-OTA HRP spiked with OTA at different concentrations (*slow2*). Once again the excess of antibody solution is removed with PBS.

Finally the last solution introduced is TMB. TMB requires a high flow rate that is achieved in the last pump, to be able to saturate. Figure 2.21 illustrates the immunoassay that occurs in the reaction

chamber. Between each step there is a washing step with 1.2µL of PBS. As demonstrated the colorimetry can be detected visually and accessed through optical microscopy.

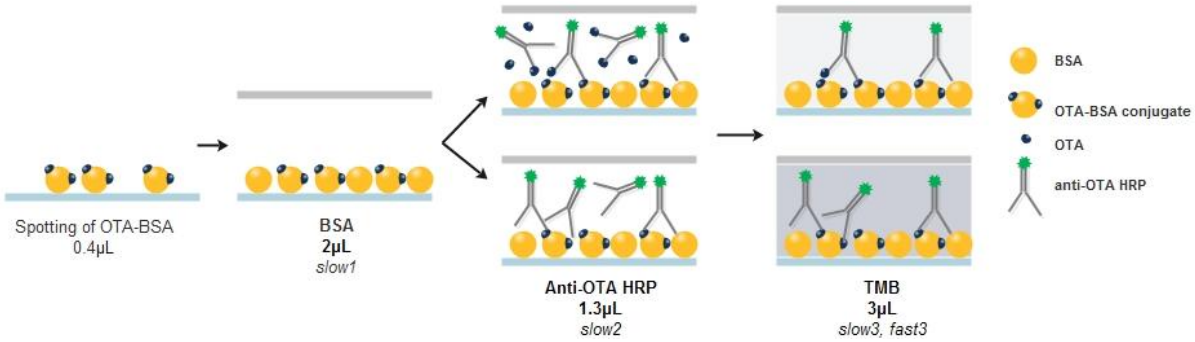

Figure 2.21 Schematics of the icELISA protocol. The duality of the assay corresponds to an OTA spiked solution (top) and a reference sample without OTA (bottom)

The introduction of all solutions is made manually, by approaching the pipette tip to the inlet near the reaction chamber. After passing through the entire device the liquid gets to the outlet. At this point no more liquid can enter the chip or be pumped, since all the pumps are full. The normal assay time is 15 minutes.

2.3.2.1 Extract experiments

Besides studying the OTA immunoassay in PBS it was also included an immunoassay where the OTA was obtained from corn for salmon feed extracts (corn for salmon feed production kindly supplied by EWOS, Norway, within the framework of the FP7-SME EU DEMOTOX project - project reference 604752).

In order to obtain the OTA, there is the inclusion of an extraction step that allows the collection of two samples. One without OTA that represents the reference and another contaminated with 1000ng/mL of OTA. Within the protocol mentioned previously, these solutions will integrate the role of free OTA that it is added to the anti-OTA HRP solution. Therefore, the competition between free OTA and the immobilized OTA on the surface is preserved. The OTA samples only differ in the origin.

2.3.3 Data analysis

The microscopic images presented in this work were acquired in an Olympus CKX-41 microscope (coupled with a digital camera Olympus XC30) and AmScope (coupled with a digital camera AmScope MD600) for the dye experiments and immunoassays, respectively.

After the immunoassays the colorimetry is detected by optical microscopy. TMB flows in the final step of the assay and by reacting with HRP produces a colored product. The intensity of the signal is proportional to the amount of HRP present, which in turn is inversely proportional to the concentration of OTA tested.

The produced signal is acquired by a camera connected to the optical microscope (Amscope). The analysis of the intensities obtained for different OTA concentrations is performed in the software ImageJ. Since considering a colorimetric detection the results can be studied by calculating the light absorbance. The sample is excited by a light source and the regions of interest selected, namely for the background and for a spotted area. The mean intensities are obtained for these regions and the transmittance (T) is calculated. The relation between transmittance and absorbance is given by Beer-Lambert law,[46]

$$A = -\log(T) = -\log\left(\frac{\mathrm{I}}{\mathrm{I}_0}\right) \quad (15)$$

For analysis the absorbance can then be plotted in function of the OTA concentration tested. It is important to include in this study the existing error for each measurement. The error bars used were obtained from the standard deviation of the data.[61]

3 RESULTS AND DISCUSSION

This chapter summarizes the main results obtained, and also allows explaining some of the decisions made during the experimental work period. Section 3.1 describes the evolution o the process of optimizing the capillary conditions. Namely the importance of surface treatment. Section 3.2 continues with the study of those conditions for some of the solutions used during the immunoassay, such as PBS and BSA. Section 3.3 details the results obtained in the OTA immunoassay and the process of analysis of the signal detected. Lastly, section 3.4 describes the inclusion of a module responsible for the sequential introduction of several solutions needed for an assay, and some details important for its proper operation.

According to concepts explained in sections 1.3 and 1.4, surface properties are very important in capillary devices. Therefore, it is important to mention that for all the experiments that will be explained in this section the glass cleaning protocol was always performed like described in section 2.1.

3.1 Optimization of capillary conditions

3.1.1 *Slow* and *fast* pump behavior

In order to have a working capillary system it is really essential to assure the right surface conditions, in terms of cleanness and surface treatment. Taking this into account, a significant amount of experiments performed in the capillary structures allowed to understand that there are critical conditions that need to be addressed.

In this subsection, all the experiments were performed by inserting a food dye diluted in water. Before addressing the results it is important to clarify how the data was obtained and analyzed.

In order to study the capillary conditions, while the fluid flowed through the structures the time was registered. Since the dimensions of the structure are known the time was recorded whenever the liquid turned the channel's curve (as shown in Figure 3.1). After collecting all the position and time data, the velocity can be calculated.

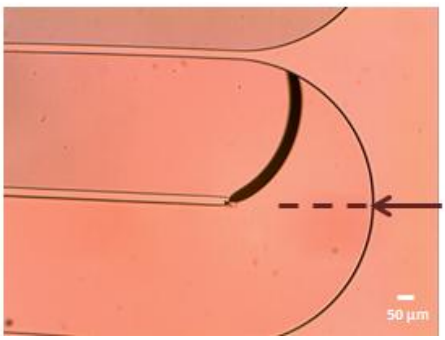

Figure 3.1 Microscopic view of the fluid front turning, for a dye experiment. Once the front reaches the region marked the time is registered (Olympus10x).

The first set of experiments was performed in version1 (illustrated in Figure 2.14 in section 0). In this case, the PDMS structure was sealed with a lamella with 100µm thickness (100 deckgläser, Hirschmann laborgeräte). The sealing was performed by carefully assembling the PDMS with the thin glass. Once the assembly is done, the structure is tested by inserting the dye.

As can be observed in Figure 3.2, the fluid took about 50minutes to fill half of the first pump. As it is easy to understand, the time consumed for performing any assay in a chip with this behavior it is not acceptable for a PoC device. The main reason behind the considerable slow velocity of this structure has to do with the level of impurities in the glass used. These lamellas are very thin, becoming very difficult to clean them. In fact, rinsing these substrates with water has a high probability of fracture.

Therefore the need of a more robust substrate emerged. The alternative chosen was a glass substrate with 0.5mm thickness (Corning glass 7059), that allows cleaning. Thus, from this point on, all the experimental work was performed with PDMS-corning glass devices.

Yet again observing Figure 3.2, for a chip sealed with the new substrate, the behavior of the fluid front is more promising. To reach the same distance, the system takes less then 10minutes instead of 50minutes registered for the lamella glass.

As mentioned in previous sub-sections surface treatments can be used to change the surface of a material and improve some of its characteristics, for instances hydrophilicity. Since capillarity depends on the hydrophilicity of the surfaces in contact with the fluid, including a cleaning step is determinant. This way, besides changing the substrate, the cleaning takes a major importance in the performance demonstrated (Figure 3.2).

Thus, before sealing the device, the glass slide was subjected to a wet cleaning step and to UV/Ozone treatment for 6minutes. Once both treatment and sealing are complete the structure is ready for testing.

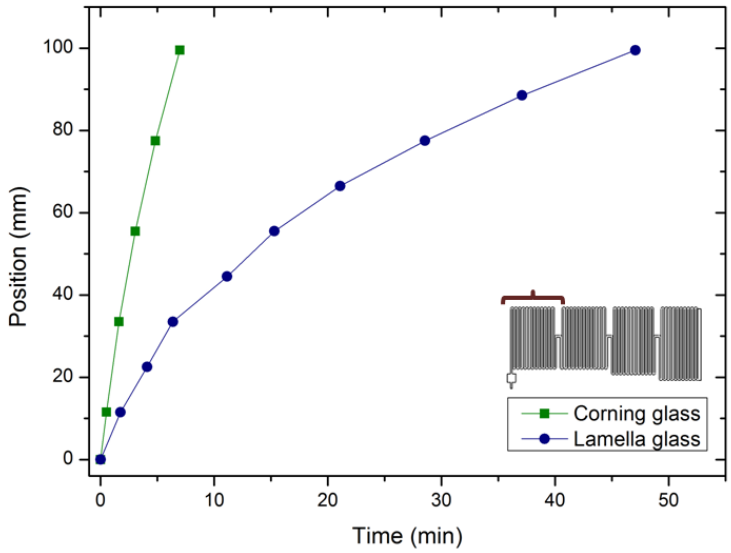

Figure 3.2 Comparison of the filling time response of the structure, for the dye, with two different glass substrates

Referring to the working principle of the device there's one more interesting aspect to study, which is the advancement of the fluid meniscus. In sub section 1.2.5 the meniscus position in function of time was defined by equation13. As both the equation and the plot in Figure 1.11 suggest the position of the capillary meniscus shows a square-root of time dependence. In order to confirm this aspect the fit curve of the position data points for the experiment in corning glass was obtained (shown in Figure 3.3). As can be observed the same dependence of time is depicted for the experimental data points. The parameter a corresponds to $h\sqrt{\frac{\Delta p_s}{6\mu}}$.

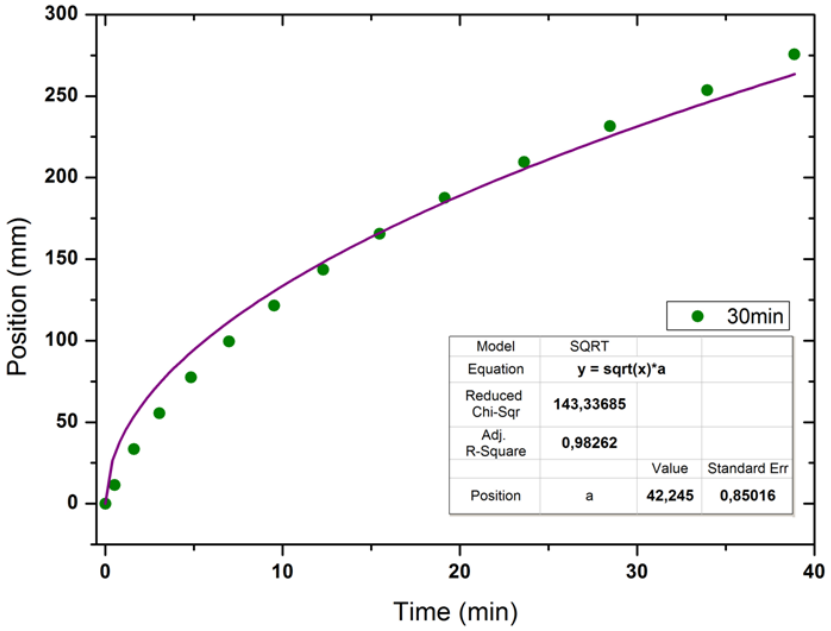

Figure 3.3 Representation of the position as a function of time with the respective fit curve, for a dye experiment in a *slow* pump

In addition it was studied the behavior of a slow and fast pump separately. Figure 3.4 demonstrates the position and velocity profiles for both pumps. As expected, in a fast pump the velocity reaches higher values, illustrating the effect produced by the passageways (according with the working principle described in section 2.2.1).

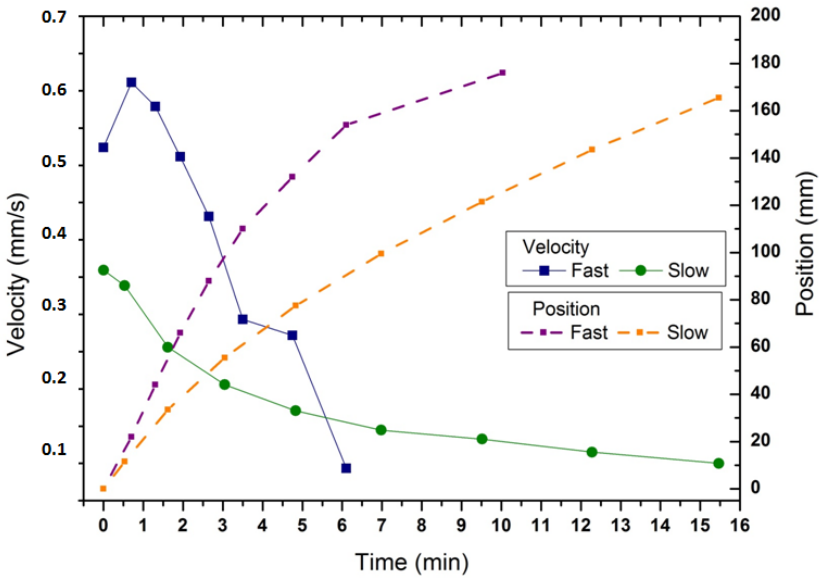

Figure 3.4 Velocity and position profiles for a dye experiment, in a *slow* and a *fast* pump

Considering that the passageways behave like valves that keep the liquid trapped and only allow it to flow when the fluid front reaches those spots (as illustrated in Figure 3.5). This figure also demonstrates the profile of the fluid front that behaves similarly to a laminar flow.

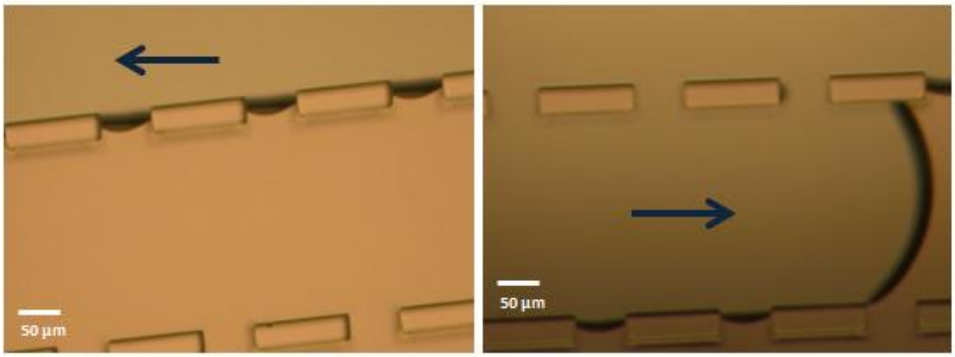

Figure 3.5 Microscopic view of a fast pump before (left) and after (right) the passage of the dye's fluid front (Olympus20x)

Figure 3.6 demonstrates a structure, composed of a slow and a fast pump, completely covered by the food dye.

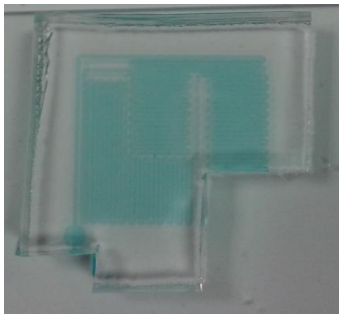

Figure 3.6 Photograph of a structure used to test the effect of sequential pumps, with the dye solution

3.1.2 Surface treatment

The following point of interest has to do with the effect of surface treatment. As mentioned before, all the glass slides used to seal the structures were subjected to a UV/Ozone treatment. In several trials, the glass slides were treated, the structure sealed and stored. The exact time between the treatment and the experiment was not controlled, however it was at least 2h.

It is also important to refer that the treatment of PDMS was considered and tested. The tests were realized in structures in which a single PDMS and glass and a sealed PDMS-glass structure were subjected to the UV/Ozone treatment. For the single PDMS and glass the sealing occurred immediately after the treatment. The significance of these experiments was to verify the influence of treating both structures separately or already sealed. It was noticed that in both cases the liquid was not able to enter the channels, and if entered it got stuck in the beginning of the structure.

Therefore the hypothesis that the period of time between the glass treatment and the beginning of the experiment influenced the fluid behavior emerged. With the purpose of understanding this phenomenon various periods of time between treatment and experiment were tested, including 30minutes and 1h.

Let us consider Figure 3.7. In this graph it is represented the velocity profiles for a slow pump in four different structures. Two of these experiments were performed 30minutes after the treatment ($t_{after\ UVO\ 30min}$), whereas for the other two the waiting time before starting was 1h ($t_{after\ UVO\ 1h}$). As can be observed, this is not a trivial issue. Actually the influence of time after treatment can have significant changes in fluid flow behavior.

For the same covered distance the structures of $t_{after\ UVO\ 30min}$ show a time response of about half the ones of $t_{after\ UVO\ 1h}$. Obviously, this difference will have an impact in fluid velocity within the channel. In fact it shows that the velocities of the channels in $t_{after\ UVO\ 30min}$ can reach the 0.7-0.9mm/s.

These results are concordant with the relation described in section 1.3.1 which refers that glass by being highly hydrophilic, represents the wettable wall that induces the motion of the fluids. In fact, by treating the glass surface, besides removing any contaminants it also increases surface energy.[62]

In terms of the influence of the waiting time, after the treatment the tendency to adsorb contaminants increases.[41] These contaminants affect the contact angle of the liquids in the surface, and consequently its hydrophilicity.[63] The longer the time before the experiment, the higher the probability of accumulation of dust and particulate that affects the properties of the glass.

Considering a slow pump in the beginning of the structure, it is desired to have a reasonable value of velocity to assure the fluid flow through all the length. Therefore, if it takes too long to fill the first pump it will be difficult to guarantee that there will be enough driving force to pull all the solutions.

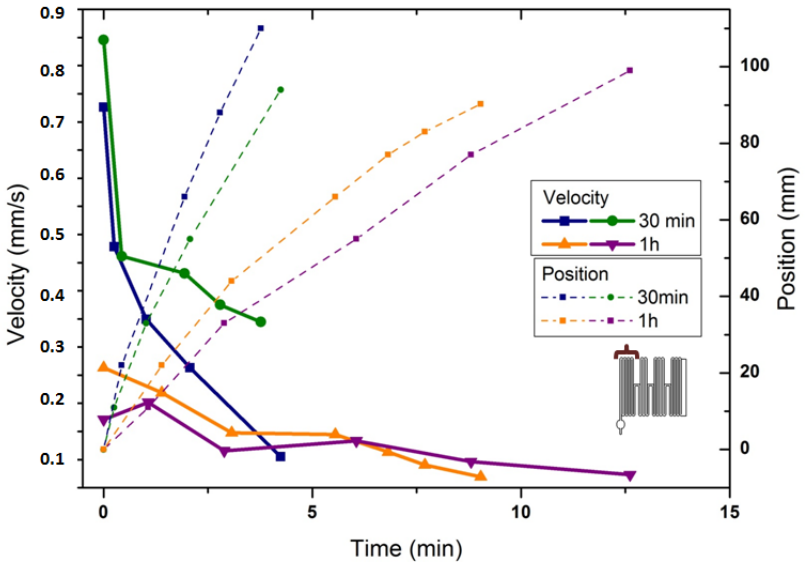

Figure 3.7 Velocity and position profiles of the fluid front, for the dye solution, in a *slow* pump, for experiments starting 30minutes and 1h after the UV/Ozone treatment of the glass slide

Taking these results into account for the following experiments the waiting time chosen was 30minutes. Considering that the properties change with time and level of contamination, for the next experiments the devices were stored in vacuum, for about 25minutes before being used. It was possible to verify that the vacuum environment with the absence of contaminants and dust helps to maintain the hydrophilic characteristics.

3.1.3 Pump sequence

It is still important to understand the effect in fluid flow of placing different pumps in sequence. In order to investigate this effect, several tests were made in the capillary chip version4. According to the following graphic (Figure 3.8), the blue and the orange regions correspond to the slow and fast pump, respectively, for two experiments. As the fluid starts to flow through *slow1* velocity decreases, lasting about 5 minutes. Once the fluid front reaches *fast1* the fluid speed increases. As the fast pump gets filled the speed tends to decrease, however the variation is smaller than in the case of a *slow* pump.

When reaching *slow2* the velocity keeps decreasing, now in a more pronounced way. At last the front gets to the final pump and once again there's a boost in speed. With the accumulation of resistance, in *fast2* the speed decreases until the fluid reaches the end of the microfluidic structure.

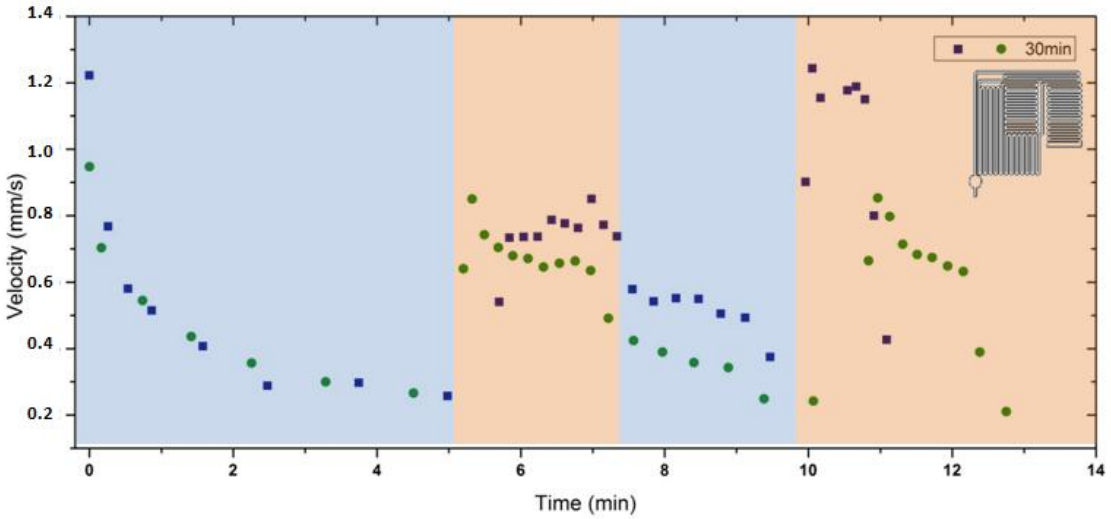

Figure 3.8 Velocity profile of the fluid front, for the dye solution, in the complete structure (version4) for experiments starting 30minutes after the UV/Ozone treatment of the glass slide

The comparison of the behavior of this structure with a similar one in literature[26] reveals that by sequentially placing different pumps is possible to simulate the necessary velocities for diverse assay steps.

Another important concept in microfluidics is flow rate. Flow rate corresponds to the volume of a certain fluid that flows through a surface in a certain period of time. Therefore it depends on the properties of the fluid and on the geometry of the channel. As mentioned in section 1.3.5, flow rate can be approximated to the product of the flow velocity with the cross-sectional area of the channel (equation12).

Knowing the dimensions of the channel (width 300μm and height 50μm) is possible to calculate the flow rate for the pumps, particularly to each data point. The relation between velocity and flow rate is illustrated in Figure 3.9. The graph obtained refers to one of the experiments (green data) mentioned in Figure 3.8.

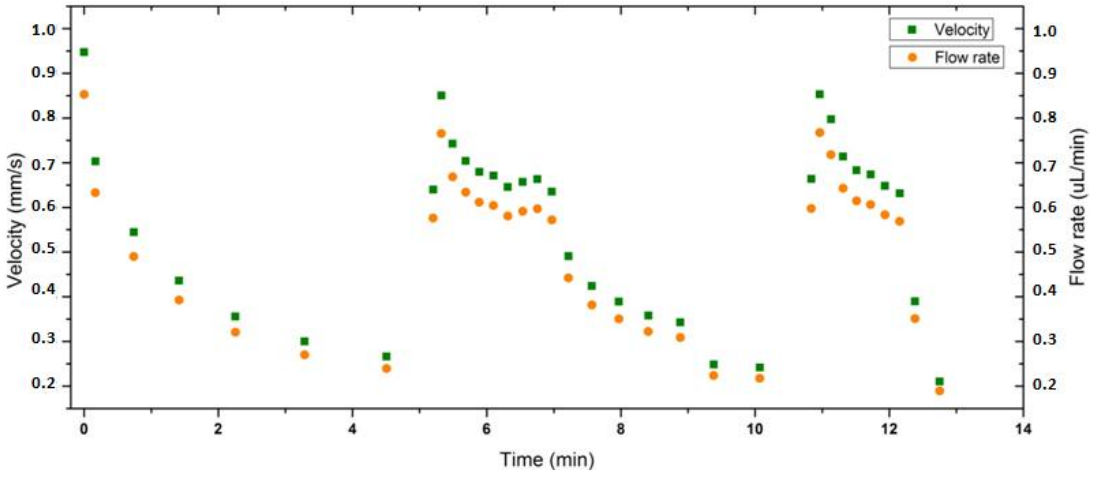

Figure 3.9 Comparison of fluid velocity and flow rate, for the dye solution, in the complete structure (version4) for experiments starting 30minutes after the UV/Ozone treatment of the glass slide

The results presented in this graph show that the flow rate is proportional to velocity, and can be obtained by multiplying the cross sectional area of the channel (0.015mm^2) in each point. Therefore the behavior of both curves is the same. Once again is possible to detect the existence of a sequence of *slow, fast, slow* and in the end another *fast* pump.

The conversion from fluid velocity to flow rate is important, because velocity by itself only depends on the fluid behavior. While studying flow rate we are also including the geometry of the structure in which the assays are performed. Besides, the flow rate can give information about the volume of solutions necessary to fill each pump, according with the flowing time.

3.2 The importance of PBS

An additional aspect to take into consideration is the fluid itself. In a way that fluids have different properties, including mass, density and viscosity.

PBS is a saline buffer used frequently in dilutions. Since the preparation of the solutions for the immunoassays was done with PBS, this solution was chosen to study the response of the capillary system to a more viscous fluid. The results illustrated in Figure 3.10 show that changing the fluid has a great impact in the performance of the device. Regarding the introduction of PBS, as can be observed, the velocity and consequently flow rate suffer a reduction when compared with the previous experiments with the diluted food dye.

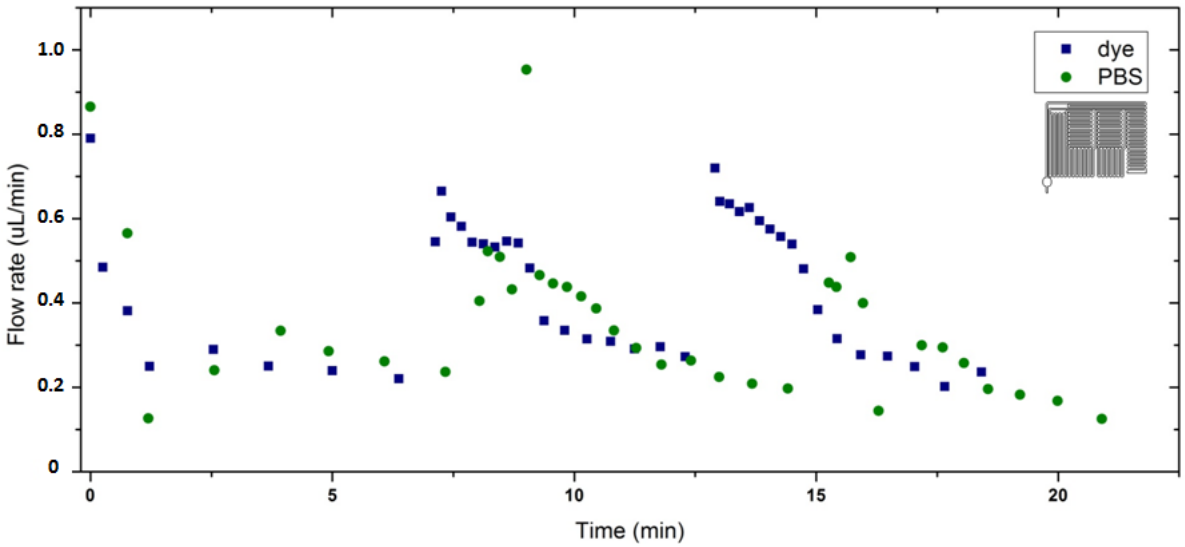

Figure 3.10 Comparison of flow rate in the complete structure (version5) for experiments with dye and PBS, starting 30minutes after the UV/Ozone treatment of the glass slide

Another solution worth studying is 4% BSA prepared by diluting it in PBS. At a particular high concentration, PBS viscosity suffers a change. In fact when comparing to PBS only, BSA has a resulting addition of viscous properties. According with equations 8, 10, the viscosity of a fluid has a

proportional relation with the hydraulic resistance produced, which in turn affects fluid velocity.[62] As a result the higher the level of viscosity of a solution the higher the resistance to fluid motion.

Though the process of inserting the BSA in the capillary systems revealed to be not viable for the defined conditions. Considering all the previous results, a parameter that had already shown to change the behavior of the device is the time between UV/Ozone treatment and experiment. For this reason and in order to manipulate the system to be able to receive the BSA that is essential for blocking the reaction chamber during the assay, the new time tested was 5 minutes ($t_{after\ UVO\ 5min}$).

In the current conditions, the capillary response was experienced, for comparison, with PBS and BSA. So, as Figure 3.11 shows, for $t_{after\ UVO\ 5min}$ the BSA solution manages to enter the channel, yet it takes too long to fill the first pump. The graph demonstrates that the high level of viscosity of the BSA solution results in a considerable decrease of capillary flow rate.

In fact the average flow rate for this solution is 0.17μL/min. In contrast, the PBS response shows higher values of flow rate, for instances for the slow pump it reaches 0.90μL/min. This flow rate is 4 times the value for BSA and 3 times the flow rate for PBS with $t_{after\ UVO\ 30min}$ (0.29μL/min).

It is also important to mention that several experiments were realized between 5 and 10minutes after the treatment and showed a similar behavior. However, for longer times the response is the one described ahead.

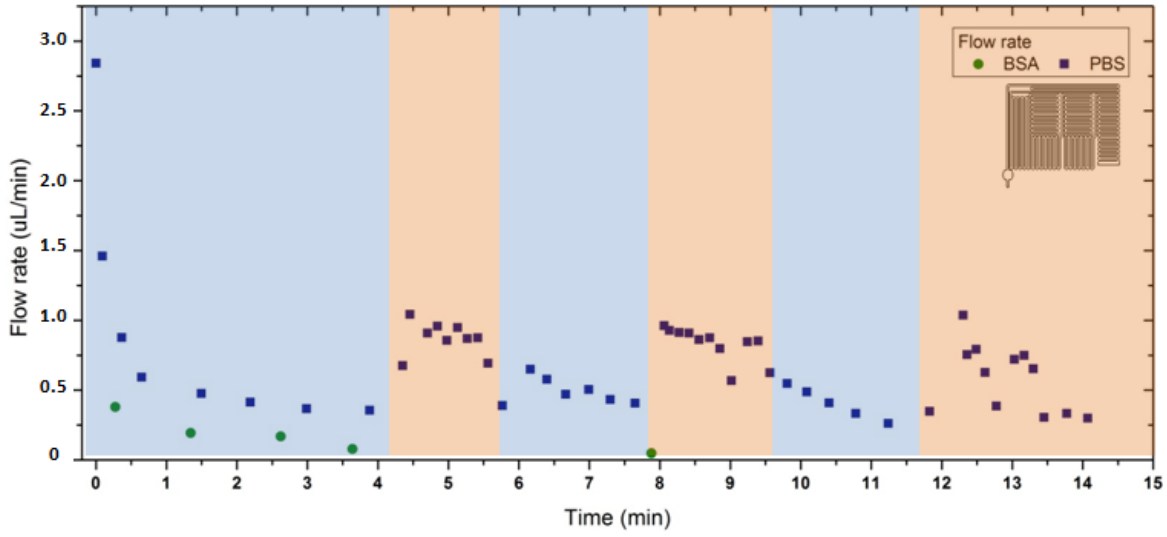

Figure 3.11 Comparison of flow rate in the complete structure (version5) for PBS and BSA experiments starting 5minutes after the UV/Ozone treatment of the glass slide

Taking into consideration the low flow rates for BSA and the adequate PBS response, the hypothesis of placing a small volume of PBS before the insertion of BSA came up. Therefore before the introduction of the 2μL of BSA, 0.5μL of PBS was introduced. In fact, as demonstrated in Figure 3.12 the PBS+BSA combination allows having an average flow rate of 0.38μL/min. The outcome

demonstrates that being PBS less concentrated than BSA, and therefore less viscous, it facilitates fluid motion.

This phenomenon has to do with the driving force that controls fluid flow. As mentioned in section 1.3.1 surface tension is the motor in capillary driven flows, since it produces capillary pressure. Δp_s depends on the contact angles that the fluid has with the walls that constitute the channels, and is mainly controlled by the glass surface (as indicated by equation14). Assuming that the contact angles of both solutions don't differ to much the main factor that contributes to the difference in flow rates is the viscosity of the fluids. This assumption is verified by the results presented in this graph.

In what refers to the volume of PBS chosen, 0.5µL is the enough amount to give the increment in terms of flow rate and it doesn't fill excessively the pumps intended for other solutions.

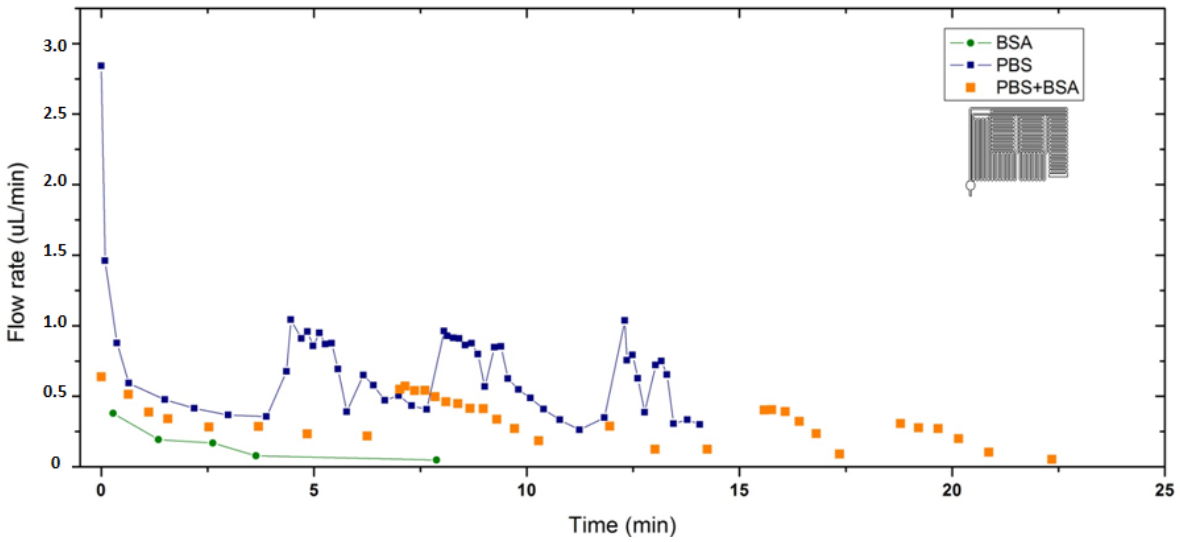

Figure 3.12 Comparison of flow rate in the complete structure (version5) for PBS, BSA and BSA with PBS experiments starting 5minutes after the UV/Ozone treatment of the glass slide

Taking these results into account, the best conditions to the realization of the OTA immunoassay were defined. Summing up, to perform an immunoassay in the proposed capillary system, it's fundamental to start the experiments between 5 and 10minutes after the glass treatment. As well it is necessary to insert 0.5µL of PBS before the introduction of BSA.

3.3 OTA immunoassay

After all the preparation of the capillary chips and of the solutions, everything is ready for the capillary icELISA. As described before the OTA immunoassay consisted in a step of spotting the OTA-BSA in the reaction chamber region, in the PDMS structure. Then and after evaporation the PDMS was sealed with the treated glass slide. Figure 3.13 shows a microscopic view of the spot after it dried and the structure sealed. The sketch of the reaction chamber indicates the orientation of the pictures. The decision of spotting the conjugate OTA-BSA instead of flowing it along with the other solutions was made, due to the existence of a spatially defined region for signal reading.

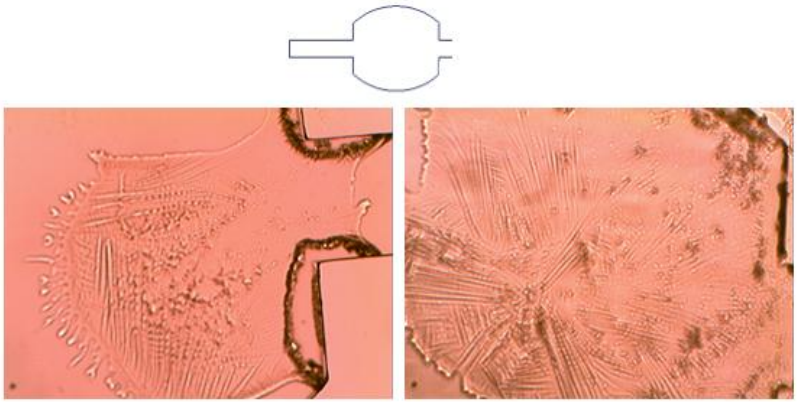

Figure 3.13 Microscopic view of the spotted OTA-BSA in the reaction chamber (bottom) and schematic representation of the reaction chamber (top) (AmScope 10x)

Afterwards and following the assay protocol, the combination of PBS with BSA was introduced. The BSA has the function of blocking the surface in order to avoid non specific adsorption of the antibodies that could influence the colorimetric result. Then there is a washing step with PBS, anti OTA labelled with HRP, PBS again and at last the TMB solution.

The general assay time is around 25 to 30 minutes, depending not only on the capillary system, but also in the time spent in inserting manually the solutions into the inlet. The latter's influence in the pumps flow rates is represented in Figure 3.14. The information about the last fast pump is not represented on the plot, nevertheless the fluid front reached the end of the structure in every one of the assays.

By observing and comparing this graphic with the previous results, it is detectable the presence of some abrupt peaks where the data points should follow the trend defined previously. These peaks are represented in the exact regions that correspond to the introduction of the next solution. This means that in this step there are several events that can influence the capillary response. Namely if the next solution is inserted when the previous completely enter the structure, in this case the fluid front stops until the next fluid starts flowing. Or if the next solution is inserted while the previous one is still flowing but almost finishing, for this case, the fluid can maintain its motion without interruption. Nevertheless, none of these events produce drastic changes in the fluid flow, since the time spent in the insertion process wasn't significant.

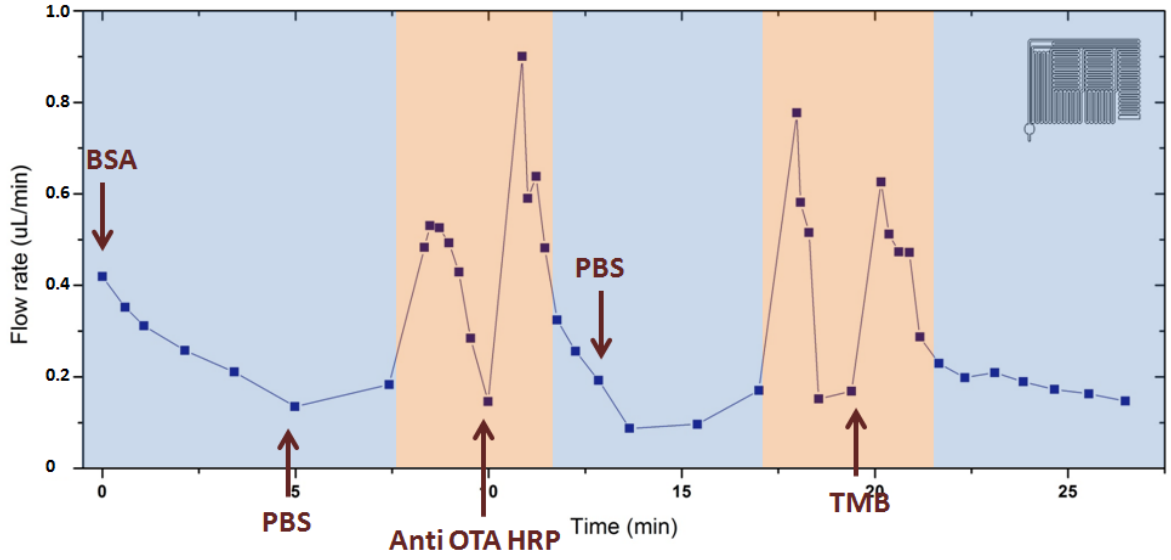

Figure 3.14 Representation of the flow rate for the OTA immunoassay in the complete structure (version5), including the data points where the solutions were inserted, for solutions prepared in buffer

The flow rates and filling times associated with the icELISA protocol performed are summarized in Table 3.1. Both the average velocities and the filling times were calculated as the average values of three sets of experiments, and the flow rate was obtained according to Equation12.

Table 3.1 Sequential steps of the capillary icELISA protocol

Immunoassay step	Filling time (min)	Average velocity (mm/s)	Flow rate (µL/min)	Volume (µL)
Blocking (BSA)	8	0,34	0,306	2
Washing (PBS)	3.5	0,53	0,477	1.2
Target antibody (anti-OTA HRP)	7	0,29	0,261	1.5
Washing (PBS)	3	0,42	0,378	1.2
HRP substrate (TMB)	5 3	0,18	0,162	3

The objective of the immunoassay tests in the capillary system was to investigate the ability to detect various concentrations of OTA. Particularly concentrations of 2ng/mL that correspond to the regulatory limit of OTA for wine.[51] The detection is possible through colorimetry. Therefore, in order to analyze the results several images obtained from an optical microscope are studied.

One way of doing a quantitative colorimetric measurement is by using a using a light source in the visible range and measure absorbance. In this case, the sample is excited by a light source of intensity I_0, and the amount of light that it is transmitted I is measured.

In order to obtain these parameters, let us consider the example of a microscopic image obtained after the immunoassay. So the mean intensity values correspondent to intensity of the amount of

light transmitted and the one emitted by the source are identified through selecting a region of interest in two places of the reaction chamber. Since the interest is to quantify the color produced during the reaction of the immunoassay species, I is obtained in the colored region, corresponding to the area where the OTA-BSA was spotted, and I_0 outside the spot region, as a reference.[46] (As illustrated in Figure 3.15)

The mean intensity values are obtained in the software ImageJ. With these values the transmittance and absorbance can be calculated, for each experiment.

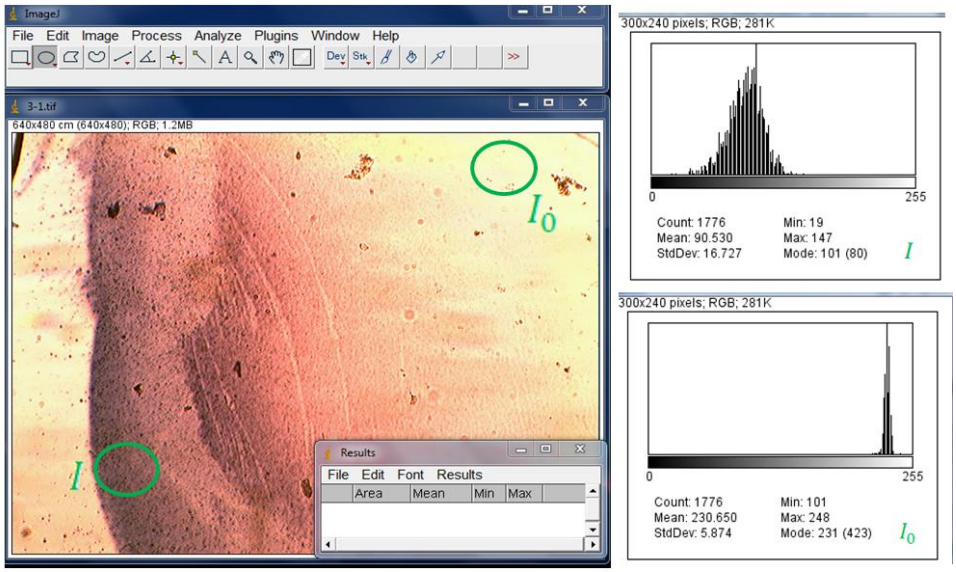

Figure 3.15 Representation of the selection of the region of interest and calculation of the mean intensity values for the selected regions (Amscope)

For the first set of experiments the spotting of OTA-BSA was made with a diluted solution with a concentration of 50µg/mL. However the colorimetric signal for the reference measurement (0ng/mL) was not sufficiently strong, leading to the decision of spotting a solution with a higher concentration, namely 1mg/mL. After this modification the results showed a significant increase in intensity.

In Figure 3.16 it is represented the absorbance plot in terms of the OTA concentration present. The microscopic images allow making a visual connection between the immunoassay results and the absorbance analysis. According to these results, the increase in OTA concentration leads to a decrease of signal, namely in absorbance.

This can be explained by the fact that for a OTA concentration of 0ng/mL, when the solution of anti-OTA HRP is introduced in the system, all the antibodies are free to bind to the OTA-BSA conjugates immobilized in the PDMS structure. An experiment in these conditions is considered the reference, since the objective is to detect the presence of OTA contamination. (The immunoassay protocol is described in Figure 2.21)

Whereas in a case where in the anti-OTA HRP solution is added a certain concentration of OTA, the antibodies will have the tendency to bind to the free OTA in solution. This way, when inserting this

combination in the capillary system, the amount of free anti-OTA HRP able to bind to the immobilized antigens is smaller. Resulting in a decrease in signal detected. Consequently, since the competition increases, the higher OTA concentration mixed with the anti-OTA HRP the less signal can be detected.[50]

So, as expected the results show a decrease in colorimetry for an increase in OTA concentration. Since the signal decreases, and the colors are less intense the ratio between the transmitted and the emitted light increases. Therefore the transmittance of the system is enhanced. Consequently the absorbance level tends to be smaller. The error bars were obtained with the standard deviation of the results, for a number of samples per concentration of 6,5,7 and 5 for the 0, 1, 10 and 100ng/mL, respectively.

These experiments showed that the capillary system is sensitive enough to allow the detection of OTA concentration within the regulatory limits.[51]

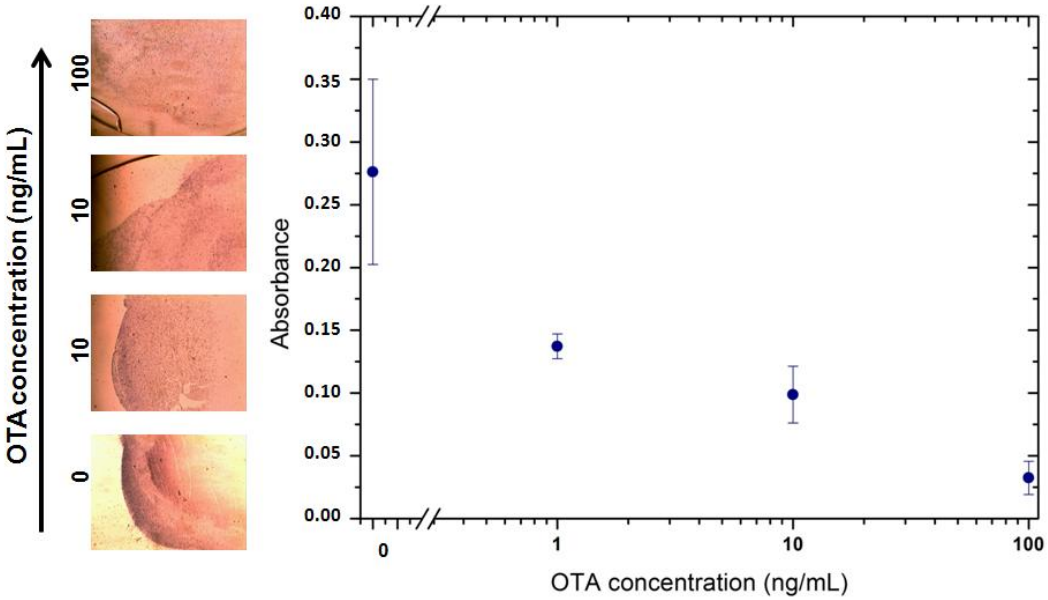

Figure 3.16 Comparison of colorimetric icELISA results, in the capillary system obtained by optical microscopy (Amscope 10x), for several OTA concentrations prepared in buffer: microscopic view (left) and absorbance results (right). The error bars were obtained with n=6,5,7 and 5 respectively for each concentration

One of the main interests on working with a colorimetric detection was to study the future possibility of importing the data with a cell phone camera. The reaction chamber format and dimensions are explained by this interest.

In Figure 3.17 some photographs from the results of the immunoassay are distributed according to the OTA concentration. As can be observed the relation between colorimetry and concentration confirms the results depicted in Figure 3.16. The reference shows an intense color that decreases until it is barely distinguishable, when reaching the 100ng/mL concentration.

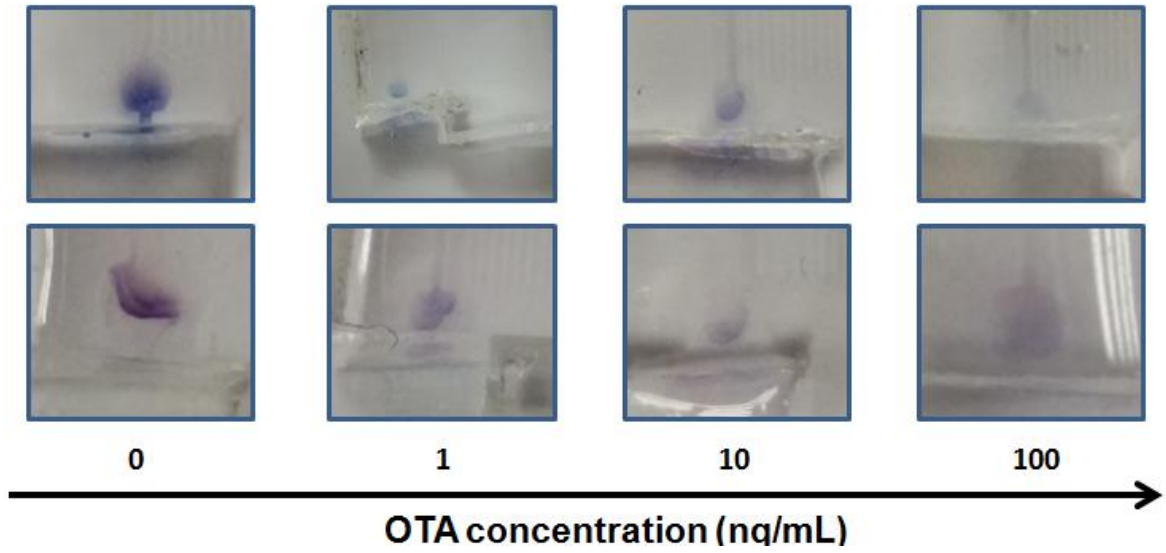

Figure 3.17 Comparison of colorimetric icELISA results in the capillary system obtained through a cell phone camera, for several OTA concentrations prepared in buffer

One more aspect worth mention is the non-homogeneity of the colorimetric region within the reaction chamber. The color is detected in the region where the OTA-BSA was spotted and therefore where the anti-OTA HRP binding took place. However the format of the drop and the evaporation influence the distribution of the color (as demonstrated in Figure 3.13). It was shown that this fact doesn't affect the results, because in the image software only a small region of interest is selected. However when envisioning the possibility of an external camera, e.g. cell phone the area should be more homogeneously distributed.

In order to study the quality of the acquired images of both cameras the absorbance was calculated (Figure 3.18). The differences are not drastic, however the decrease in absorbance depicted in the images obtained by the cell phone camera (8.0MP) is in concordance with the lack of resolution of the acquired photos. Not being able to perfectly define the reaction camber structure nor the colored spotted area. Therefore, to consider this acquisition method in the future, more work should be done in order to avoid loss of information.

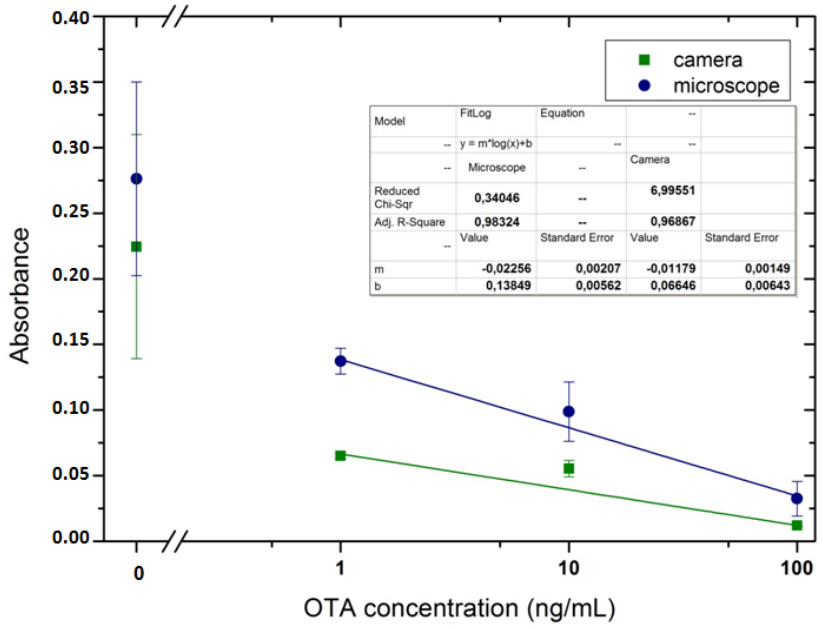

Figure 3.18 Comparison of the colorimetric detection, of several OTA concentrations prepared in buffer, for optical microscopy (Amscope 10x) and cell phone camera (8.0MP). The error bars (standard deviation) of the camera data were obtained with 3 samples per concentration value

3.3.1.1 OTA quantification in artificially contaminated feed samples

The extract experiments differ from the previous immunoassays in source medium of OTA. As mentioned before the OTA is extracted from a corn sample. Upon the collection of the OTA, this is added to the anti-OTA HRP solution in order to make the desired concentrations. For the extract experiments, only a reference and one contaminated solutions were tested, respectively 0 and 1000ng/mL. The immunoassay is performed in the same way, with the same volumes and the signal detection is also colorimetric.

As illustrated in Figure 3.19, the sensitivity of the OTA detection for the extract experiments decreases when comparing with the previous tests that detected OTA in PBS. This can be seen by the reduction in the absorbance values in both cases. In fact for the reference concentration, in the PBS medium the signal is almost the double than for the extract.

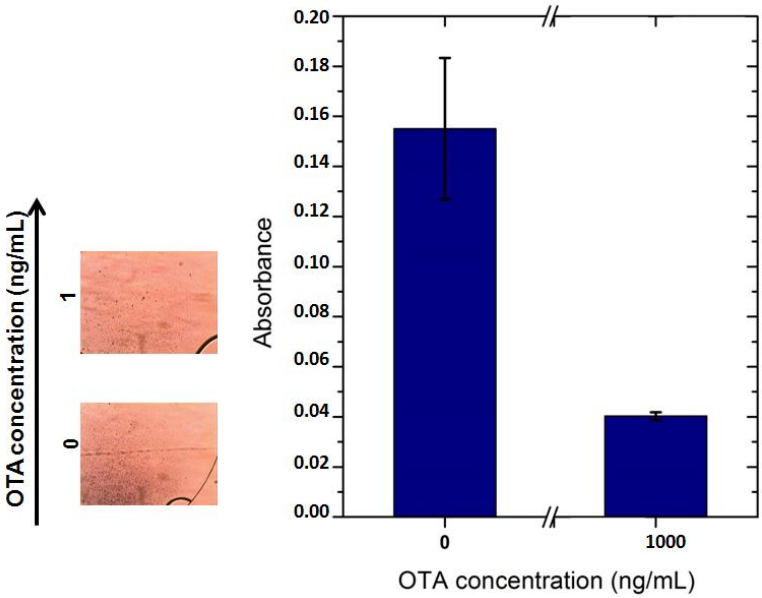

Figure 3.19 Comparison of colorimetric icELISA results in the capillary system obtained by optical microscopy (Amscope 10x), for several OTA concentrations in the extracts: microscopic view (left) and absorbance results (right). The error bars (standard deviation) were obtained with 3 samples per concentration value

Figure 3.20 shows that in both cases, the signal is almost undetectable by eye unlike the experiments in PBS, in which it was possible to notice even the 100ng/mL. These results are concordant with previous work, and can be expected by the influence of matrix components that can interfere with the binding of anti-OTA HRP to OTA-BSA or with their reactivity.[50]

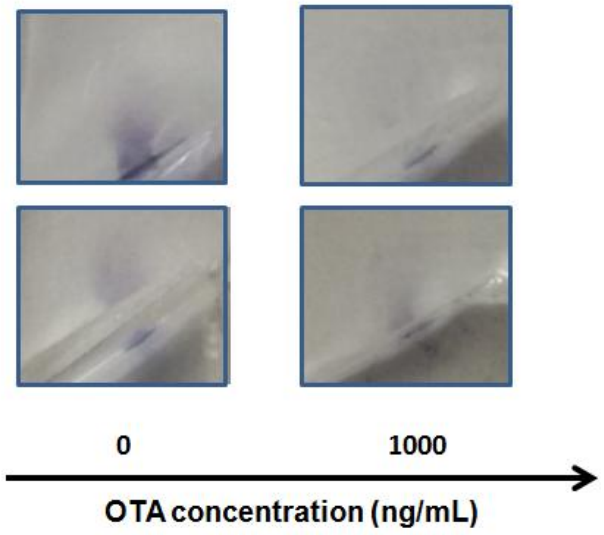

Figure 3.20 Comparison of colorimetric icELISA results in the capillary system obtained for the extract experiments, through a cell phone camera

As described for the assays with OTA in PBS, for these experiments a comparison between the microscope and camera images was made (Figure 3.21). In this case, the signal detected is significantly lower, becoming difficult to visualize the reaction area. As expected, the standard

deviation obtained for the reference results is larger. This has to do with the fact that for the 1000ng/mL concentration the intensity of the signal in the spotted area is almost equal to the non-spotted. Therefore the variation between measurements is less significant. On other hand, for the reference concentration, the signal intensity is higher, allowing a larger variation between measured intensities.

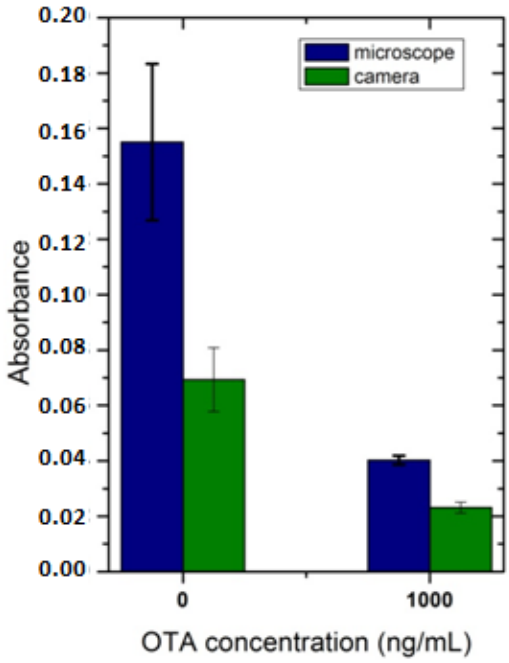

Figure 3.21 Comparison of the colorimetric detection, of two OTA concentrations in the extract experiments, for optical microscopy (Amscope 10x) and cell phone camera (8.0MP).). The error bars (standard deviation) of the camera data were obtained with 3 samples per concentration value

3.4 Sequential delivery

The main objective of studying the hypothesis of having in the structure a module for sequential insertion of solutions was to facilitate this process and decrease the level of interference from the user. The module adopted was based on a previous work, where it was demonstrated the insertion of solutions from 3 inlets, without mixing them before entering the device.[14]

For the immunoassay studied in this work it was required that the module had 6 inlets, including one for the initial 0.5µL of PBS. The only user intervention required is to place all the solutions near the inlets. Figure 3.22 shows one example of inlet cuts that allow storing the solutions before they enter the device.

However, several requisites need to be checked, like the fact that the liquids can't mix outside the device, in case this happens the solutions get contaminated one with another and the purpose of maintaining the sequence is lost. Another important requisite is assuring that while placing the solutions that the valve near the inlets is covered, otherwise the difference of pressure will induce the next solution to flow before the previous was completely consumed.

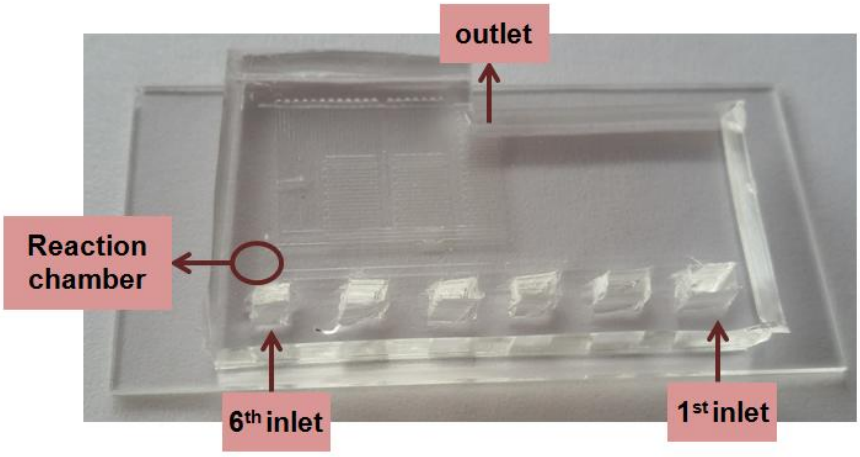

Figure 3.22 PDMS-glass capillary device with the sequential insertion module

Also the sealing of the device needs to be carefully assessed, in order to make sure that all the PDMS is in contact with the glass to avoid the presence of air that leads to leakage. At last, since the solutions are in contact with air they are prone to evaporate while waiting for the previous ones to flow, for that reason is important to place a larger volume then the one required for the assay

The possibility of the autonomous insertion of solutions can facilitate the development of the immunoassay and even solve some variabilities in the flow rates introduced by the manual insertion (as explained in Figure 3.14).

While testing the module, sometimes it was possible to make all the inlets fill the structure correctly. However, in most of the experiments the module didn't work properly. Therefore, there are still some improvements to be done, in terms of reproducibility of the experiments, that can be explained by the reasons presented before.

In the overall, the results illustrate the possibility of performing complex immunoassays using microfluidic devices that don't require external equipments to flow the solutions. Capillary pumps with a manual insertion of solutions demonstrate to be a viable tool for OTA detection.

4 CONCLUSIONS AND FUTURE WORK

The development of this work has opened the perception to the impact of conditions that need to be assured before using capillary microfluidic devices. The main claims of this project are not only the development of a capillary chip capable of performing a multi-step immunoassay, but also the recognition of the critical points for its use.

In capillary microfluidic devices several conditions, like chip characteristics, surface properties, contaminations are known to influence the chip behavior.

With respect to the chip characteristics, it was shown that the fabrication of the device is important for the performance. According with the results demonstrated, within the fabrication of the SU-8 mold a correct UV exposure is determinant for the correct definition of the mold. Obtaining a well defined mold is a primary step for a good definition of the PDMS channels. This point is relevant to assure that the channels have the proper geometry. In fact, it the geometry is not constant the fluid front can follow not regular behavior. Since channels geometry influences capillary pressure the flow rate can also be affected.

Still considering the chip properties, the surface treatment can be considered one of the main discoveries associated with this work. The previous knowledge on surface properties like surface tension and contact angle was important as a starting point. Thus, PDMS is known for having a larger contact angle and therefore for its hydrophobicity. In contrast, glass is described in the literature as being hydrophilic. This information, led to the hypothesis of cleaning and treating glass in order to remove contaminants. However, after treatment it was noticed that not only glass gets cleaned but also there is an increase in its hydrophilic characteristics. The improvement in hydrophilicity is important, because induces a decrease in contact angle that in turn increases capillary pressure and flow rate.

Still it was also important to understand that these properties are dependent on the factor time, especially when considering a PoC application. The results demonstrate that for periods of time superior to 30minutes the flow rates reach low values. However when starting the experiments about 5minutes after the glass treatment and the sealing, the fluid front reaches the outlet in a shorter period of time.

About this circumstance it also important to mention the influence of fluid viscosity. For a fluid with a higher coefficient of viscosity, the hydraulic resistance to fluid motion is higher and consequently the flow rate decreases. Therefore when testing the capillary structure with solutions like PBS and BSA that has to be a compromise between viscosity and time after UV/Ozone treatment.

In terms of the capillary structure used for the immunoassays, the sequence of pumps showed to be adequate. For adsorption steps, when the molecules within the sample are required to be immobilized in the surface or to bind with other species the flow rate needs to be slow enough to

allow these reactions. Thus, in order to reach a slow flow rate, a straight microchannel (*slow* pump) was considered. On the opposite, for washing steps where the species that didn't bind should be removed the flux should be stronger. Therefore in these cases the channels used were composed of passageways (*fast* pump) that increased flow rate.

The sequence of pumps used was shown to be efficient in introducing the right fluxes for the different steps that composed the assay. Therefore, the capillary system proposed is sensitive enough to allow the detection of relevant concentrations of OTA.

Addressing the main conclusion of this project, it was shown that it is possible to customize a capillary microfluidic system to a specific application. In the perspective of PoC devices a capillary system can be very relevant, since it performs without the need of external equipments improving portability of the system. Besides, a short time analysis was provided (25-30min) only requiring the user intervention in loading the sequential solutions in the inlet.

4.1 Future work

In terms of future developments, there are some improvements that can be done in the structure, namely in the initial module. It was proven that the module that contained the 6 inlets worked, however in terms of reproducibility the experiments realized with this sequential insertion of solutions. The main issue is to reproduce the conditions and timings that were performed manually and that showed good results.

Another interesting working point to consider for the sequential delivery is the incorporation of loading regions in the inlets where the solutions could be stored until the beginning of the experiments. In order to avoid the evaporation resultant from the waiting time, and as well to decrease the dependence of manual handling in the insertion. When considering this chip in the perspective of a PoC device, these modifications can be important for the portability.

Considering the interest of creating a PoC device based in the capillary microfluidic device proposed in this thesis, there is one more issue to consider. It was demonstrated that the wetting properties vary significantly with the time between treatment and assay. When designing a commercial product there is no way of anticipating the on shelf time, thus, this chip would not be viable. Therefore there is a particular interest on finding a way of ensuring the stability of the wetting properties.

For some of the experiments with longer waiting times the devices were stored in vacuum. Which showed that the structures maintained their hydrophilic properties better than the ones saved in a petri dish in the lab environment. These results can be the starting point for the consideration of storing the device in a case with a sterile environment, until being used.

Hence the main consideration for these capillary devices is the integration on a kit, that could already contain the solutions and that only required the insertion of the sample to test.

Considering the possibility of producing a PoC diagnosis device for biomedical applications, it is important to add a set of experiments in order to study the behavior of the device to biological fluids, such as serum and blood.

At last for the detection and analysis of the assay results, the possibility of giving the user the opportunity of acquiring the signal leads to the use of the cell phone. If using a colorimetric signal the definition of the cell phone cameras is able to detect it, as demonstrated previously. Therefore, it could be interesting to create an app that could perform the same analysis than the software ImageJ, and give a quantitative result. This way, and considering an user-friendly software the end user could place the sample, the device perform the assay and by taking a picture the result would be given. As designing a device intended to be of PoC use having all functions needed for processing and analyzing the sample included is of great interest.

BIBLIOGRAPHY

[1] S. Haeberle and R. Zengerle, “Microfluidic platforms for lab-on-a-chip applications,” *Lab Chip*, vol. 7, no. 9, p. 1094, 2007.

[2] L. R. Volpatti and A. K. Yetisen, “Commercialization of microfluidic devices,” *Trends Biotechnol.*, vol. 32, no. 7, pp. 347–350, 2014.

[3] MarketsandMarkets, “Microfluidics Market by Application, Material, Diagnostic & End User - 2020,” 2015.

[4] A. K. Yetisen and L. R. Volpatti, “Patent protection and licensing in microfluidics,” *Lab Chip*, vol. 14, no. 13, p. 2217, 2014.

[5] L. Gervais and E. Delamarche, “Toward one-step point-of-care immunodiagnostics using capillary-driven microfluidics and PDMS substrates.,” *Lab Chip*, vol. 9, no. 23, pp. 3330–3337, 2009.

[6] P. N. Nge, C. I. Rogers, and A. T. Woolley, “Advances in Micro fl uidic Materials , Functions , Integration , and Applications,” 2013.

[7] D. Juncker, H. Schmid, U. Drechsler, H. Wolf, M. Wolf, B. Michel, N. De Rooij, and E. Delamarche, “Autonomous microfluidic capillary system,” *Anal. Chem.*, vol. 74, no. 24, pp. 6139–6144, 2002.

[8] M. Zimmermann, P. Hunziker, and E. Delamarche, “Valves for autonomous capillary systems,” *Microfluid. Nanofluidics*, vol. 5, no. 3, pp. 395–402, 2008.

[9] M. Zimmermann, H. Schmid, P. Hunziker, and E. Delamarche, “Capillary pumps for autonomous capillary systems,” *Lab Chip*, vol. 7, no. 1, pp. 119–125, Dec. 2007.

[10] M. Hitzbleck and E. Delamarche, “Advanced capillary soft valves for flow control in self-driven microfluidics,” *Micromachines*, vol. 4, no. 1, pp. 1–8, 2013.

[11] L. Gervais, M. Hitzbleck, and E. Delamarche, “Capillary-driven multiparametric microfluidic chips for one-step immunoassays,” *Biosens. Bioelectron.*, vol. 27, no. 1, pp. 64–70, 2011.

[12] C. C. Lin, J. H. Wang, H. W. Wu, and G. Bin Lee, “Microfluidic Immunoassays,” *JALA - J. Assoc. Lab. Autom.*, vol. 15, no. 3, pp. 253–274, 2010.

[13] P. Novo, V. Chu, and J. P. Conde, “Integrated optical detection of autonomous capillary microfluidic immunoassays: A hand-held point-of-care prototype,” *Biosens. Bioelectron.*, vol. 57, pp. 284–291, 2014.

[14] P. Novo, F. Volpetti, V. Chu, and J. P. Conde, “Control of sequential fluid delivery in a fully autonomous capillary microfluidic device.,” *Lab Chip*, vol. 13, no. 4, pp. 641–5, 2013.

[15] P. Novo, G. Moulas, D. M. F. Prazeres, V. Chu, and J. P. Conde, “Detection of ochratoxin A in wine and beer by chemiluminescence-based ELISA in microfluidics with integrated photodiodes,” *Sensors Actuators, B Chem.*, vol. 176, pp. 232–240, 2013.

[16] J. C. McDonald and G. M. Whitesides, “Poly(dimethylsiloxane) as a material for fabricating microfluidic devices,” *Acc. Chem. Res.*, vol. 35, no. July, pp. 491–499, 2002.

[17] L. Gervais, N. De Rooij, and E. Delamarche, “Microfluidic chips for point-of-care immunodiagnostics,” *Adv. Mater.*, vol. 23, no. 24, 2011.

[18] P. B. Lillehoj, F. Wei, and C.-M. Ho, “A self-pumping lab-on-a-chip for rapid detection of botulinum toxin.,” *Lab Chip*, vol. 10, no. 17, pp. 2265–2270, 2010.

[19] R. Safavieh and D. Juncker, “Capillarics: pre-programmed, self-powered microfluidic circuits built from capillary elements.,” *Lab Chip*, vol. 13, no. 21, pp. 4180–9, 2013.

[20] D. J. Beebe, G. a Mensing, and G. M. Walker, “Physics and applications of microfluidics in biology.,” *Annu. Rev. Biomed. Eng.*, vol. 4, pp. 261–286, 2002.

[21] G. Bracco and B. Holst, *Surface science techniques*, vol. 51, no. 1. 2013.

[22] H. Bruus, “Theoretical microfluidics,” *Physics (College. Park. Md).*, vol. 18, no. 33235, p. 363, 2008.

[23] D. Juncker, “Capillary Microfluidic Systems for Bio / Chemistry,” 2002.

[24] B. J. Kirby, *Micro-and Nanoscale Fluid Mechanics: Transport in Microfluidic Devices*. Cambridge University Press, 2010.

[25] G. Li, Y. Luo, Q. Chen, and J. Zhao, “a Capillary-Pressure-Based Air Pump for Nanoliter Liquid Handling in Microfluidic Devices,” *15th Int. Conf. Minituarized Syst. Chem. life Sci.*, pp. 918–920, 2011.

[26] P. Novo, “Advanced optical lab-on-chips for point-of-care applications,” 2014.

[27] T. M. Squires, “Microfluidics Fluid physics at the nanoliter.pdf,” vol. 77, no. July, 2005.

[28] K. . Oh, “Lab-on-chip (LOC) devices and microfluidics for biomedical applications,” in *Mems for Biomedical Applications*, 2012, pp. 151–157.

[29] J. Chen, S. Liao, M. Liu, J. Lin, T. Sheu, and M. Jr., “Surface Tension Flows inside Surfactant-Added Poly(dimethylsiloxane) Microstructures with Velocity-Dependent Contact Angles,” *Micromachines*, vol. 5, no. 2, pp. 116–138, 2014.

[30] W. van der Wijngaart, “Capillary pumps with constant flow rate,” *Microfluid. Nanofluidics*, pp. 1–9, 2014.

[31] L.-J. Yang, T.-J. Yao, and Y.-C. Tai, “The marching velocity of the capillary meniscus in a microchannel,” *J. Micromechanics Microengineering*, vol. 14, no. 2, pp. 220–225, 2003.

[32] K. V. Sharp, R. J. Adrian, J. G. Santiago, and J. I. Molho, “Liquid Flows in Microchannels,” *MEMS Handb.*, pp. 6.1–6.38, 2002.

[33] J. D. Zahn, *Methods in Bioengineering: Biomicrofabrication and Biomicrofluidics*. Artech House, 2014.

[34] R. Safavieh, A. Tamayol, and D. Juncker, “Serpentine and leading-edge capillary pumps for microfluidic capillary systems,” *Microfluid. Nanofluidics*, vol. 18, no. 3, pp. 357–366, 2014.

[35] P. Tabeling, *introduction to Microfluidics*. Oxford University Press, 2005.

[36] J. A. Jofre-reche, J. Pulpytel, F. Arefi-khonsari, U. Pierre, and C. Paris, “Adhesion Improvement of Polydimethylsiloxane (Pdms) By Surface Treatment With Two Different Atmospheric,” vol. 5001, pp. 2–4.

[37] J. Landers, *Handbook of Capillary and Microchip Electrophoresis and Associated Microtechniques*. 2008.

[38] A. Oláh, H. Hillborg, and G. J. Vancso, “Hydrophobic recovery of UV/ozone treated poly(dimethylsiloxane): Adhesion studies by contact mechanics and mechanism of surface modification,” *Appl. Surf. Sci.*, vol. 239, no. 3–4, pp. 410–423, 2005.

[39] L. Gervais, “Capillary Microfluidic Chips for Point-of-Care Testing : from Research Tools to Decentralized Medical Diagnostics,” 2011.

[40] “Essential Points of UV/Ozone Dry cleaning.” [Online]. Available: http://www.senlights.com/gijyuu/drycleaning/drycleaning.html. [Accessed: 27-Sep-2015].

[41] W. R. Birch, “Cleaning Glass Surfaces,” in *Sol-Gel Technologies for Glass Producers and Users*, Springer Science & Business Media, 2004, pp. 30–35.

[42] Y. Temiz, R. D. Lovchik, G. V. Kaigala, and E. Delamarche, “Lab-on-a-chip devices: How to close and plug the lab?,” *Microelectron. Eng.*, vol. 132, pp. 156–175, 2015.

[43] A. D. Stroock and G. M. Whitesides, “Components for integrated poly (dimethylsiloxane) microfluidic systems,” *Electrophoresis*, vol. 23, no. 20, pp. 3461–3473, 2002.

[44] K. Anwar, T. Han, and S. M. Kim, “Reversible sealing techniques for microdevice applications,” *Sensors Actuators, B Chem.*, vol. 153, no. 2, pp. 301–311, 2011.

[45] J. Lee and P. Li, “Development of immunoassays for protein analysis on nanobioarray chips,” in *Microfluidic devices for biomedical applications*, 2013, pp. 445–464.

[46] D. Li, *Encyclopedia of microfluidics and nanofluidics*, vol. 1. 2008.

[47] “ELISA Encyclopedia,” 2015. [Online]. Available: http://www.elisa-antibody.com/ELISA-Introduction/ELISA-types. [Accessed: 13-Oct-2015].

[48] E. P. Meulenberg, “Immunochemical methods for ochratoxin A detection: a review.,” *Toxins (Basel).*, vol. 4, no. 4, pp. 244–66, 2012.

[49] L. Al-Anati and E. Petzinger, “Immunotoxic activity of ochratoxin A.,” *J. Vet. Pharmacol. Ther.*, vol. 29, no. 2, pp. 79–90, Apr. 2006.

[50] R. R. G. Soares, P. Novo, a. M. Azevedo, P. Fernandes, M. R. Aires-Barros, V. Chu, and J. P. Conde, “On-chip sample preparation and analyte quantification using a microfluidic aqueous two-phase extraction coupled with an immunoassay,” *Lab Chip*, vol. 14, no. 21, pp. 4284–4294, 2014.

[51] European Commision, “Commission Regulation (EC) No 1881/2006, Setting maximum levels for certain contaminants in foodstuffs,” *Off. J. Eur. Union*, vol. 2006, no. 1881, pp. 5–24, 2006.

[52] A. H. C. Ng, U. Uddayasankar, and A. R. Wheeler, “Immunoassays in microfluidic systems.,” *Anal. Bioanal. Chem.*, vol. 397, no. 3, pp. 991–1007, 2010.

[53] “Alconox Laboratory Detergent,” 2015. [Online]. Available: http://www.2spi.com/item/z01200/. [Accessed: 06-Oct-2015].

[54] U. H. V Ii, “Chapter II Process equipment and experimental techniques,” *Film*, pp. 19–53, 2000.

[55] Elveflow, “SU-8 mold lithography,” 2015. [Online]. Available: http://www.elveflow.com/microfluidic-tutorials/soft-lithography-reviews-and-tutorials/introduction-in-soft-lithography/su-8-mold-lithography/. [Accessed: 22-Aug-2015].

[56] MicroChem, “NANO ™ ANO ™ SU-8 Negative Tone Photoresist Formulations 50-100.”

[57] Sigma-Aldrich, “Ochratoxin A from Petromyces albertensis, ≥98% (HPLC) |.” [Online]. Available: http://www.sigmaaldrich.com/catalog/product/sigma/o1877?lang=pt&region=PT. [Accessed: 29-Oct-2015].

[58] Sigma-Aldrich, “Ochratoxin A−BSA conjugate from Aspergillus ochraceus.” [Online]. Available: http://www.sigmaaldrich.com/catalog/product/sigma/o3007?lang=pt&region=PT. [Accessed: 29-Oct-2015].

[59] ImmuneChem, “Ochratoxin A Antibody, HRP,” 1998. [Online]. Available: http://www.immunechem.com/?app=product&act=look&type_id=16&id=192. [Accessed: 27-Oct-2015].

[60] Thermo Fisher Scientific, “TMB-Blotting Substrate Solution,” 2015. [Online]. Available: https://www.thermofisher.com/order/catalog/product/34018. [Accessed: 27-Oct-2015].

[61] G. Cumming, F. Fidler, and D. L. Vaux, “Error bars in experimental biology.,” *J. Cell Biol.*, vol. 177, no. 1, pp. 7–11, Apr. 2007.

[62] Promimic, “A Hydrophilic Surface,” 2015. [Online]. Available: http://www.promimic.com/index.php/research/improved-hydrophilicity. [Accessed: 21-Oct-2015].

[63] Z. Li, Y. Wang, A. Kozbial, G. Shenoy, F. Zhou, R. McGinley, P. Ireland, B. Morganstein, A. Kunkel, S. P. Surwade, L. Li, and H. Liu, “Effect of airborne contaminants on the wettability of supported graphene and graphite.,” *Nat. Mater.*, vol. 12, no. 10, pp. 925–31, Oct. 2013.

Appendix A. RUN SHEET - Microchannel Fabrication

A.1 Fabrication of the aluminum hard mask

Step 1 - Cleaning of glass substrate in a wet bench

- Rinse with IPA
- Immerse in hot Alconox (>5min)
- Rinse with water

Step 2 – Aluminum deposition – Magnetron sputtering
Machine: Nordiko 7000

Step 3 – Photolitography for the definition of the microfluidic pattern

- Spin coat of photoresist in track 2 (Recipe 6/2)

Coating Parameters	
1st step	Dispense PR and spinning 800 rpm for 5s
2nd step	Spin at 2500 rpm for 30s
3rd step	Soft bake at 85°C for 60s

- Litography DWL

- Development of the exposed sample in track 1 (Recipe 6/2)

Development Parameters	
1st step	Bake at 110°C for 60s
2nd step	Cool for 30s
3rd step	Developer for 60s

- Inspection of the sample in the microscope

Step 4 – Aluminum wet etch at the wet bench

- Immersion of the sample in Gravure Aluminium Etchant (for 5min)
- Wash with water and dry
- Inspection of the sample in the microscope

Step 5 – Resist strip at the wet bench

- Wash with acetone
- Wash with water and dry
- Inspection of the sample in the microscope

4.2 Fabrication of the SU-8 mold

Step 6 – Preparation of the Si substrates

- Wash the Si substrates with acetone
- Immersion of the substrates in Alconox in hot strip (65°C for 20min)
- Wash with water and dry
- UVO-cleaner (for 25min)

Step 7 – Spin coating of SU-8 in the laminar flow camera

- Spin coat the substrate with SU-8
    - Step1: 500 rpm, 100 rpm/s, 10s
    - Step2: 2300 rpm, 300 rpm/s, 37s

Step 8 – SU-8 mold

- Soft bake 65°C for 3min and 95°C for 8min
- Expose the substrate to UV for 25s
- Post exposure bake 65°C for 1min and 95°C for 7min
- Develop the SU-8 by immersion in PGMEA for 6 min with agitation
- Wash with IPA and dry
- Hard bake 150°C for 15min
- Inspection of the sample in the microscope and in the profilometer

4.3 Fabrication of the PDMS microfluidic device

Step 9 – Preparing the PDMS mixture

- Mix PDMS with curing agent (1:10)
- Degas under vacuum in the desiccators

Step 10 – Preparation of the glass substrates

- Wash the glass substrates with acetone
- Immersion of the substrates in Alconox in hot strip (65°C for 20min)
- Wash with water and dry
- UVO-cleaner (for 11min)

Step 11 – PDMS and mold

- Wash mold
- Inject the PDMS mixture in the mold
- Cure for 1.30h at 70°C
- Remove the PDMS from the mold
- Seal the PDMS structure with glass substrate